INTERACTIVE CONTROL ENGINEERING
Principles and Applications

Volume 20 Motion Control, Robotics, and Autonomous Systems

CHAPTER 2

Lane Keeping on a Kinematic Bicycle: Speed Dependence of a Stanley Path-Following Loop

Pages 24–53

Edited by John D. Hedengren

How to cite this chapter. "Lane Keeping on a Kinematic Bicycle: Speed Dependence of a Stanley Path-Following Loop," in *Motion Control, Robotics, and Autonomous Systems*, John D. Hedengren, Ed., vol. 20 of *Interactive Control Engineering: Principles and Applications*. Advanced Process Solutions, LLC, 2026, ch. 2, pp. 24–53.

The page numbers in this file are those of the printed volume.

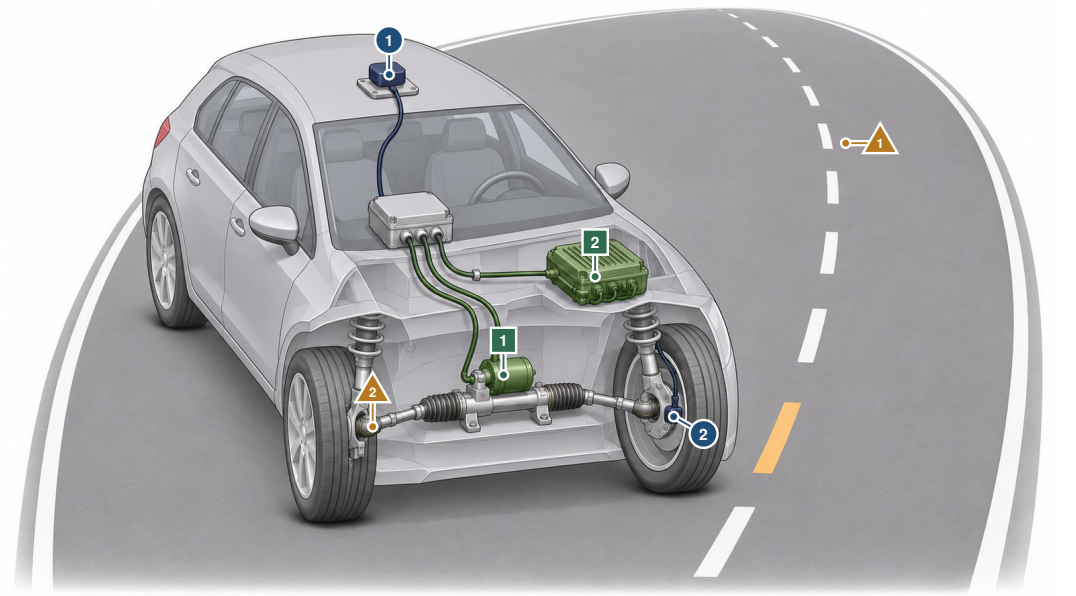
The app for this chapter
https://apmonitor.com/apps/lane-keeping/

The volume online: contents, other chapters and citation records
https://apmonitor.com/apps/books/v20-motion-robotics/#lane-keeping

Copyright © 2026 Advanced Process Solutions, LLC. All rights reserved. Produced by Advanced Process Solutions, LLC.

CHAPTER 2

Lane Keeping on a Kinematic Bicycle: Speed Dependence of a Stanley Path-Following Loop



The controller moves 1 the steering motor on the rack, which turns the front wheels
2 the drive and the brakes, which set the speed

The controller reads 1 the position module on the roof: where the car sits across the lane
2 the wheel-speed sensor: how fast the car goes

What disturbs it 1 the bend ahead, known from the road map, which the steering must follow
2 a steering linkage set slightly crooked

Notice the motor on the rack between the front wheels: every correction the controller makes passes through it, with its lag and its end stop. Illustration, not to scale.

IN PLAIN TERMS **Keeping a Car in Its Lane at Any Speed**

The main idea. A lane-keeping controller turns the front wheels to hold a car in the middle of its lane. The faster the car goes, the more a turn of the wheels swings it sideways. So the controller asks for less steering at higher speed.

The challenge. That trick cannot speed up the steering motor, which always takes the same short time to respond. A fast car travels farther in that time. No amount of correction holds a bend tighter than the wheels can turn, and a crooked wheel leaves the car off center.

Why it matters. Systems that help drivers stay in their lane are now fitted to a large share of new cars.

THREE WAYS TO READ THIS CHAPTER

Explore	8 min	the first page, the fact on lane departure warning (Section 2.1), the history of the steering law (Section 2.2), the try-it segment and the fact on one step of gain (Section 2.6), and the key points
Study	60 min	the whole chapter with its three pause points and the twelve exercises at its end
Practice	20 min	the first page, the results (Section 2.6), Technology in Practice (Section 2.7), Limitations (Section 2.8) and the open challenge

The control question A steering angle sets a yaw rate in proportion to the speed. How much of that the Stanley law cancels by construction, and what limits one fixed tuning once it has?

Learning objectives

- Derive the two closed-loop poles of the linearized Stanley loop and explain why only one is free of speed.
- Predict the standing offset left by a missing curvature feedforward and by a misaligned steering linkage.
- Compute the gain at which the rack lag destabilizes the loop, and explain why the sampled controller lowers it.
- Tell an actuator that cannot deliver the required angle from a badly tuned loop.
- Compare the Stanley law with a predictive controller that estimates the misalignment, and name the model error that undoes it.

Prerequisites Sections 1.4.2, 1.4.5, 1.6.2 and 1.6.4. Section 1.6.3 is needed only for the predictive controller.

The app https://apmonitor.com/apps/lane-keeping/

See also Volume 7, Chapter 9 for a vehicle whose stability is set by its speed and Volume 7, Chapter 10 for tire forces at the friction limit. Volume 9, Chapter 4 for offset-free predictive control with an estimated bias.



2.1 Introduction

Most loops in a process dynamics and control course regulate a scalar measurement against a scalar setpoint, and the plant between the actuator and the measurement is a transfer function that a step test can identify [1]. Lane keeping is constructed differently. The error is not read from an instrument, it is computed by projecting a point on the vehicle onto a curve stored in a map, and the actuator does not act on that error directly because a steering angle sets a yaw rate rather than a lateral position. Two integrations separate the manipulated variable from the controlled variable, and the coefficient in front of both of them is the vehicle speed.

That speed dependence is the reason lane keeping merits a chapter of its own. The yaw rate a given road-wheel angle produces is $\dot{\psi} = (v/L)\tan\delta$, so a vehicle traveling at 30 m/s turns three times as fast for the same steering angle as one traveling at 10 m/s, and it covers three times the distance while any fixed-duration transient completes. A controller tuned at one speed therefore operates on a different plant at another, and the standard industrial remedy is a gain schedule indexed by the operating point [1, 2]. Volume 7, Chapter 9 treats a vehicle on which the forward speed decides whether it is stable at all.

The Stanley steering law addresses the same difficulty by construction. It divides the cross-track correction by the speed, so the correction the law requests falls as $1/v$ while the yaw rate that correction produces rises as v, and the two effects cancel. The cancellation is not an interpolated table, it is a model of the plant gain written into the control law, and it holds exactly for the correction term because the tangent of an arctangent is the identity. The cancellation does not extend to the effects the law omits. The steering actuator has a fixed lag in seconds, which at three times the speed costs three times the distance. The lateral acceleration for a given path grows as v^2. The small-angle relations behind the geometry degrade as the lateral acceleration rises.

The lane-keeping loop carries a specific set of process dynamics and control principles. Cross-track regulation on a kinematic bicycle is a double-integrating structure whose loop gain is an explicit

function of an operating variable, which makes it a concrete instance of process order and of gain scheduling. The curvature term is a feedforward from a measured reference rather than from a load, so it separates feedforward action from feedback action in a setting where the required steady input is known in closed form. The steering rack contributes actuator lag, a rate limit and an end stop, which are three distinct actuator limitations with three distinct signatures in the response. The absence of integral action in the geometric law produces a steady-state offset whose size follows from the proportional balance, and the sampled controller executing at 50 Hz places a half-sample of additional lag in the loop. The physical fundamentals are the no-slip rolling constraint at each axle, which fixes the instantaneous center of rotation and therefore the achieved curvature, and the time-scale separation between the fast heading mode and the slower lateral mode. These are the same principles that govern process loops built on material and energy balances [1, 3, 4], applied here to a system whose geometry is directly observable.

The behavior matters industrially because lane departure warning and lane keeping assistance are now fitted to a large fraction of new passenger vehicles, and their measured benefit is a reduction in police-reported crash rates rather than a tracking error in centimeters [5]. The same geometric tracker with the same three actuator limits runs on agricultural guidance, on warehouse vehicles and on mining haul trucks.

> + DID YOU KNOW? **Fewer Crashes With a Lane Warning**
>
> Police-reported crashes from 25 states of the United States, 2009 to 2015, were compared for vehicles with and without lane departure warning. After accounting for the drivers, equipped vehicles had 11 % fewer of the single-vehicle, sideswipe and head-on crashes the warning addresses, and 21 % fewer of those with injuries [5].

Textbook treatments of lateral control state the Stanley law and its stability argument and proceed to a comparison of tracking errors [6]. However, a table of tracking errors does not allow a fixed tuning to be held while the speed is tripled, and it does not separate a loop that is badly tuned from an actuator that cannot deliver the angle the road demands. The purpose of this chapter is to document a lane-keeping simulation on a kinematic bicycle and to quantify what one fixed Stanley tuning does and does not achieve as the vehicle speed, the actuator lag, the steering limit and the lateral measurement quality are each varied in turn. The kinematic bicycle and the Stanley law are both long established, and Section 1.4.5 introduces the speed-divided law on a transport cart, beside a path follower with fixed gains.

Section 2.2 traces automatic steering from buried wires to the Stanley law. Section 2.3 gives the five state equations of the simulator, its road construction, its instrument chain, its hard limits and its sample periods, so that every number in this chapter can be regenerated from the text. Section 2.4 shows that the ideal closed loop carries two real poles, only one of which is independent of speed. It derives in closed form the standing offset left by a missing feedforward, by a heading error referenced to the wrong point on the vehicle and by a misaligned steering linkage, together with the cross-track gain at which the rack lag destabilizes the loop. Section 2.5 sets out the discrete steering algorithm, the speed loop and a model predictive controller offered as a second steering law. Section 2.6 reports twelve configurations, each varying one property of the road, the vehicle or the loop, with outcomes taken from the performance metrics the application computes while it runs. One of them sets the model predictive controller against the fixed Stanley gain, and the comparison is repeated on the others. Section 2.7 names the sensors, the steering actuator and the regulation of a real system, Section 2.8 states what the model leaves out, and Section 2.9 draws the results together.

2.2 Background

Automatic steering was applied on the road well before automatic driving. Agricultural tractors and warehouse vehicles followed buried wires and painted stripes for decades using analog circuits

that closed a loop around a single lateral sensor mounted at the front of the machine. The choice of that mounting point, ahead of the axle that generates the turn, is the essential idea behind every geometric path follower that followed. Highway experiments in the second half of the twentieth century extended the same approach to passenger cars guided by cables laid in the pavement, which removed the sensing problem by building the reference into the road.

Replacing the buried reference with a camera converted lane keeping from a civil engineering problem into a control problem. Recursive estimation of road curvature and vehicle state from an image sequence, formulated as a dynamic model with the road geometry among the estimated quantities, allowed a vehicle to derive its own lateral reference at highway speed on ordinary pavement [7]. The law this chapter teaches comes from the desert race of 2005, as the history box below tells. The urban race two years later moved the emphasis to planning and to behavior around other traffic, while the lateral controller remained a geometric tracker following a curve with a known curvature [8].

> ⧖ HISTORY **A Steering Law From a Desert Race (2005)**
>
> The Defense Advanced Research Projects Agency (DARPA) launched its Grand Challenge in 2003 to spur work on unmanned ground vehicles. In the first race, in March 2004, no robot covered more than 5 % of a 142-mile desert course. The race was repeated on October 8, 2005, and five of the 23 starters finished. The winner, a robot from Stanford University, took 6 h 53 min 58 s. Its steering law pointed the front wheels parallel to the path and added the arctangent of the cross-track error, measured at the center of the front wheels, divided by the speed, so that a small error decays exponentially [9]. The law takes the orientation of the front wheels, not of the body, against the path. On the kinematic equations it was proven globally asymptotically stable, and in the desert it held the cross-track error typically under 0.1 m RMS [10].

Production lane keeping developed along a different route and for a different purpose. Lane departure warning systems measure the same lateral offset but act on the driver rather than on the steering rack, and lane keeping assistance applies a bounded steering torque that the driver can override at any time. Their value is quantified in crash rates rather than in centimeters of tracking error, and the crash rates of equipped vehicles have been compared against otherwise similar unequipped ones in police-reported data [5]. The bounded authority is deliberate. A system that performs most of the steering without visible limits reduces the driver’s supervision of it, and the pattern of use, misuse and disuse that follows from automation whose limits are not visible to its operator is one of the oldest findings in the human factors literature [11].

The control literature on path following has developed alongside both of these. Pure pursuit steers toward a point a fixed distance ahead on the path, which is simple to implement and whose stability depends on that lookahead distance in a way that was characterized early [12] and is still being refined by making the lookahead a function of speed and curvature [13]. Chapter 9 follows its routes by pure pursuit. Surveys of motion planning and control for self-driving vehicles place the geometric trackers, the kinematic model predictive controllers and the dynamic ones on a common footing [14], and direct comparisons of lateral controllers on the same vehicle and the same path report where each one begins to fail [6].

The regulatory structures of the simulator are standard ones. The Stanley law is a proportional geometric feedback with an additive feedforward and no reset action, so the steady-state offset arguments that apply to a proportional-only process loop apply here unchanged [1, 3]. The speed loop is a proportional-integral controller on a pure integrator, which is the same structure as level control on a surge drum. The actuator chain places a first-order lag, a rate limit and a position limit in series with the manipulated variable, and the stability consequence of the lag follows from the Routh criterion applied to the resulting cubic [4].

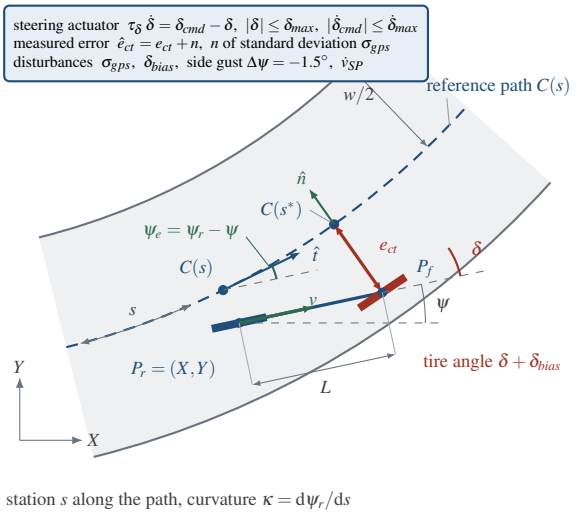


Figure 2.1 Lane keeping geometry, carrying every symbol that enters the state equations and the steering law. The cross-track error is measured at the front axle P_f and the heading error against the road direction at $C(s)$, the projection of the rear axle.

2.3 Vehicle and Road Model

The simulated system is one passenger car on one lane of a flat road. The geometry, the states, the manipulated variable, the disturbances and the measurement points are shown in Figure 2.1.

2.3.1 Signals, Units and Ranges

The signals divide into two controlled variables, two manipulated variables, five states and five disturbances, and their roles, units and permitted ranges are given in Table 2.1. Two loops act on one vehicle. The lane loop regulates a length and the speed loop regulates a speed, and either loop or both may be placed in automatic independently, so the longitudinal input can remain operator-set while the steering is closed. In the action convention of Section 1.3 the speed loop is reverse acting, because the speed rises with the acceleration command. The lane loop has no action setting in the app. Its law raises the steering angle as e_{ct} rises, and a positive steering angle lowers e_{ct}, so on e_{ct} it is a direct-acting loop.

2.3.2 Kinematic Bicycle and Steering Actuator

The two front wheels are collapsed onto the center of the front axle and the two rear wheels onto the center of the rear axle. The wheels are assumed to roll without lateral slip, so the velocity of each axle center lies along the plane of its own wheel, and that rolling constraint places the instantaneous center of rotation at the intersection of the two axle lines. With (X,Y) the rear-axle position, ψ the heading measured counter-clockwise from the world X axis, v the rear-axle speed and δ the road-wheel angle, the vehicle obeys the four relations of Equation (2.1), the kinematic bicycle.

$$\dot X = v\cos\psi, \quad \dot Y = v\sin\psi, \quad \dot\psi = \frac{v}{L}\tan\delta_{\mathrm{eff}}, \quad \dot v = a \tag{2.1}$$

where L is the wheelbase, a is the acceleration delivered to the vehicle and $\delta_{\mathrm{eff}} = \mathrm{clamp}(\delta + \delta_{bias}, -\delta_{max}, \delta_{max})$ is the angle actually taken by the tire. A misaligned linkage adds δ_{bias} between the angle the actuator reports and the angle the wheel takes, and no geometric measurement in the loop observes it. The third relation is the only steering channel in the model and it is the origin of every speed-dependent effect in the application, because the yaw rate it produces is proportional to v.

Table 2.1 Signal Roles, Units and Permitted Ranges

Symbol	Role	Unit	Range or default
e_{ct}	CV, lane loop	m	setpoint 0, band ± 0.10
v	CV, speed loop	m/s	setpoint 5 to 35, default 25
δ	MV, lane loop	rad	$\lvert\delta\rvert \le \delta_{max}$
a_{cmd}	MV, speed loop	m/s^2	-6.0 to $+3.0$
ψ_e	measured input to the law	rad	wrapped to $\pm\pi$
κ	measured input to the law	1/m	from the road table
X, Y	state, rear axle	m	free
ψ	state, heading	rad	free
v	state, speed	m/s	$v \ge 0$
δ	state, road-wheel angle	rad	$\lvert\delta\rvert \le \delta_{max}$
σ_{gps}	DV, measurement	m	0 to 0.6, default 0
δ_{bias}	DV, plant	deg	-2 to $+2$, default 0
$\dot{v}_{SP}$	DV, setpoint ramp	m/s^2	-2 to $+2$, default 0
$\Delta\psi$	DV, side gust event	deg	-1.5
Δy	DV, displacement event	m	$+0.5$ to the right
δ_{man}	operator-set steering	deg	-30 to $+30$
pedal	operator-set longitudinal	%	-100 to $+100$

The steering rack is a first-order lag with an end stop and a rate limit on its command, as shown in Equation (2.2).

$$\tau_\delta \dot{\delta} = \delta_{cmd} - \delta, \qquad |\delta| \le \delta_{max}, \qquad |\dot{\delta}_{cmd}| \le \dot{\delta}_{max} \tag{2.2}$$

where τ_δ is the rack time constant, δ_{max} is the mechanical lock and $\dot{\delta}_{max}$ is the largest rate at which the command may move. These are three separate limits with three distinct effects on the loop. The lag adds phase, the rate limit attenuates fast corrections while leaving slow ones unaltered, and the end stop removes an angle that the geometry requires. The acceleration is clamped to the traction and braking envelope, $a = \mathrm{clamp}(a_{cmd}, a_{min}, a_{max})$, and braking cannot reverse the car, so $\dot{v} = 0$ whenever $v \le 0$ and $a < 0$.

2.3.3 Road Geometry from a Curvature Profile

Every road in the application is defined by a curvature profile $\kappa(s)$ over a sequence of segments, and the four segment kinds that appear are the straight ($\kappa = 0$), the constant-radius arc ($\kappa = 1/R$ with $R > 0$ turning left), the clothoid whose curvature ramps linearly from κ_0 to κ_1 over its length, and the lateral shift, a sinusoidal curvature pulse $\kappa = (2\pi\Delta y_{seg}/\ell^2)\sin(2\pi u/\ell)$ over a segment of length ℓ with u the distance into the segment. Integrating that pulse returns the heading to its original value at $u = \ell$ and, for small heading excursions, displaces the path sideways by Δy_{seg}. Expressing a lane change as geometry rather than as a special case in the controller allows one projection routine to serve every road.

The profile is integrated into an arc-length table at a node spacing of $\Delta s = 0.5\,\mathrm{m}$ using the exact constant-curvature chord over each step, as shown in Equation (2.3).

$$\begin{aligned} \psi_{r,k+1} &= \psi_{r,k} + \bar{\kappa} h, \\ x_{k+1} &= x_k + \frac{\sin\psi_{r,k+1} - \sin\psi_{r,k}}{\bar{\kappa}}, \\ y_{k+1} &= y_k - \frac{\cos\psi_{r,k+1} - \cos\psi_{r,k}}{\bar{\kappa}} \end{aligned} \tag{2.3}$$

where h is the step to the next node or to the end of the current segment, whichever comes first, and $\bar{\kappa}$ is the curvature at the midpoint of that step. The straight-line form $x_{k+1} = x_k + h\cos\psi_{r,k}$,

Table 2.2 The Eight Shipped Roads, Given as Segment Sequences

Road	Segments (lengths in m)
Straight highway	straight 2600
Constant radius	straight 80, arc $R = 200$ for 700, straight
S-curve	straight 50, corner $R = 150$ (140), straight 40, corner $R = -150$ (140), straight 60, corner $R = 180$ (160)
Lane change	straight 70, shift $+3.5$ over 60, straight 140, shift -3.5 over 60, straight
Gentle sweep	straight 120, corner $R = 500$ (500) with 60 m spirals, straight 200, corner $R = -400$ (400) with 60 m spirals
Sudden curvature	straight 120, arc $R = 120$ for 260, straight 120, arc $R = -120$ for 260, straight
Sharp corner	straight 60, corner $R = 25$ (40), straight 120, corner $R = -25$ (40), both with 12 m spirals, straight
Challenge course	straight 40, clothoid to $1/140$ over 30, arc $R = 140$ for 130, clothoid to $-1/160$ over 40, arc $R = -160$ for 200, clothoid to 0 over 40, straight

A *corner* is a clothoid in, a constant arc and a clothoid out, with 30 m spirals unless stated. Every road is padded to 2600 m.

$y_{k+1} = y_k + h \sin \psi_{r,k}$ replaces it when $|\bar{\kappa}| < 10^{-12}$. Every road starts at the origin heading along $+X$ and is padded with a final straight to 2600 m, which is 100 s at 26 m/s. The eight shipped roads are listed in Table 2.2.

2.3.4 Cross-Track and Heading Error Definitions

The vehicle carries two independent projections onto the road table, one for the front axle and one for the rear. Each searches only the window of nodes between $s - 3$ m and $s + 25$ m around its own last station, refines the station along the tangent and reports the normal offset. At reset both trackers start from station zero, where every road begins, and a road changed under a moving vehicle carries the vehicle across at its current station. No global nearest-point search enters the loop, because on a road that doubles back the true nearest point can be a kilometer away along the path and a controller referenced to it would steer toward the wrong lane.

The front-axle position and the two errors are given by Equation (2.4).

$$\begin{aligned} P_f &= \big(X + L\cos\psi,\ Y + L\sin\psi\big), \\ e_{ct} &= \big(C(s^*) - P_f\big) \cdot \hat{n}(s^*), \\ \psi_e &= \mathrm{wrap}\big(\psi_r(s) - \psi\big), \qquad \kappa = \frac{\mathrm{d}\psi_r}{\mathrm{d}s} \end{aligned} \tag{2.4}$$

where s^* is the station of the front-axle projection, s is the station of the rear-axle projection, $\hat{n} = (-\sin\psi_r, \cos\psi_r)$ is the left normal to the path and wrap folds an angle into $[-\pi, \pi]$. The sign convention follows from the minus sign in the second relation. A positive e_{ct} means the vehicle sits to the *right* of the path, which is exactly the case that calls for a positive left steering correction, and a vehicle at $Y = -1$ m on a straight centerline reports $e_{ct} = +1$ m. A positive ψ_e means the road heads to the left of where the car is pointing. Both errors therefore call for a positive correction, which is why the law below can be written with a plus sign in front of every term.

The two reference points differ deliberately. The cross-track error is taken at the front axle, which is the point the steering angle displaces most directly, while the heading error is taken against the road direction under the vehicle. Referencing both to the front-axle projection folds the corner into the heading term, because the road heading at s^* exceeds the road heading at s by approximately $L\kappa$. Section 2.4 derives the effect on the feedforward.

Only the cross-track error is instrumented. The measurement adds a band-limited disturbance, as shown in Equation (2.5).

$$\hat{e}_{ct} = e_{ct} + \sigma_{gps}\, n, \qquad \tau_n \dot{n} = -n + \sqrt{2\tau_n}\, w \tag{2.5}$$

Table 2.3 Constants of the Plant, the Actuator and the Loops

Symbol	Meaning	Value	Adjustable range
L	wheelbase	2.9 m	2.2 to 3.8
$w/2$	lane half-width	1.75 m	1.25 to 2.5
w_{car}	vehicle width	1.86 m	fixed
ℓ_{car}	vehicle length	4.60 m	fixed
δ_{max}	steering end stop	30°	3 to 30
$\dot{\delta}_{max}$	steering rate limit	45 °/s	5 to 120
τ_δ	steering rack lag	0.10 s	0.02 to 0.60
a_{max}	traction limit	3.0 m/s^2	0.5 to 3.0
a_{min}	braking limit	−6.0 m/s^2	−6.0 to −1.0
k_e	cross-track gain	1.2/s	0.1 to 12
k_{soft}	softening constant	1.0 m/s	0.1 to 10
δ_{ff}	curvature feedforward	on	on / off
	steering law	Stanley	Stanley / MPC
T_p	MPC prediction horizon	2 s	0.5 to 4
λ	MPC move suppression	0.01	0.001 to 100
	MPC road preview	on	on / off
K_c	speed loop gain	1.2/s	0.1 to 5
τ_I	speed loop integral time	4 s	0.5 to 30
v_{SP}	speed setpoint	25 m/s	5 to 35
Δt	integration step (RK4)	0.01 s	fixed
Δt_c	control period	0.02 s	fixed
f_{log}	historian rate	20 Hz	fixed
Δs	road node spacing	0.5 m	fixed
τ_n	noise correlation time	0.35 s	fixed

The lane is therefore 3.5 m wide. Random draws are seeded per configuration, at 20260824 for the noisy-measurement configuration and at 20260901 for the challenge, so a noisy run replays identically.

where w is unit white noise, $\tau_n = 0.35$ s and the filter gain is chosen so that $\sigma_{gps} n$ carries standard deviation σ_{gps} once the filter has reached its stationary state. The noise is colored rather than white because a receiver error is correlated over a second or two instead of being independent at each sample. The heading, the road heading, the curvature and the speed reach the controller without error, and the standing offset caused by δ_{bias} is a plant misalignment rather than an instrument fault.

A lane departure is declared, and recorded in the logged data, when Equation (2.6) holds.

$$\max\left(|e_{rear}|, |e_{ct}|\right) + \tfrac{1}{2} w_{car} > \tfrac{1}{2} w \tag{2.6}$$

where w_{car} is the vehicle width and w the lane width. The flag clears again at 0.05 m of hysteresis inside the limit. Both ends of the vehicle are tested, because a front corner can cross the line while the rear axle is still inside it.

2.3.5 Parameters and Numerics

Table 2.3 gives every constant of the plant and of the shipped loops, together with the adjustable settings of the predictive controller, whose fixed weights, prices and variances are given in Section 2.5.5. The first block is the plant, the second is the actuator, the third is the controller and the fourth is the numerics. The vehicle width and length are fixed rather than adjustable, and the width enters the departure test of Equation (2.6) rather than the displayed geometry alone.

A classical fourth-order Runge–Kutta scheme advances the five states on a fixed step of 10 ms. The controller executes every 20 ms, a rate representative of a production lane-keeping electronic control unit, and the data historian logs at 20 Hz. The order of events, control and integration within a step is

the framework's (Section 1.6.1), with the controller on every second step. After each integration the app clamps v at zero and δ at the end stop and tests Equation (2.6). The 20 ms control period places a half-sample of additional lag in the steering loop, which is small against the rack lag at the default setting and is not small against the stability boundary of Section 2.4. The application opens with the vehicle on the centerline at its cruise speed, which is an equilibrium of Equation (2.1) with every derivative that should vanish equal to zero to within 10^{-12}.

2.3.6 Assumptions

No tire model and no sideslip. The kinematic bicycle assumes each wheel rolls in the direction it points, so there is no cornering stiffness, no slip angle and no load transfer, and the path curvature is exactly $\tan\delta/L$. That is a fair representation up to roughly 0.4 g of lateral acceleration on dry asphalt. Above that a real vehicle requires a slip angle to generate the cornering force, the front tires saturate before the rear, and the achieved curvature falls below the commanded one, which is understeer. The application reports the lateral acceleration as $(v^2/L)\tan\delta_{\text{eff}}$. The sharp-corner configuration of Section 2.6 demands $v^2/R = 4.0\,\text{m/s}^2$ and, with the steering pinned at its 6° limit, delivers $3.62\,\text{m/s}^2$, which is the operating region where the kinematic assumption begins to overstate the achievable curvature. The boundary between the kinematic bicycle and a dynamic bicycle carrying tire forces has been examined directly [15, 16], and the lateral dynamics that govern beyond it are standard material [17].

No coupling between the two loops. Longitudinal motion is $\dot{v} = a$ with no drag, no rolling resistance, no grade, no driveline lag and no traction budget shared between turning and braking. A real vehicle cannot brake at $6\,\text{m/s}^2$ and corner at the adhesion limit simultaneously. The speed loop in this application is therefore simpler than a real one by design, so that the configurations isolate the steering.

Perfect localization apart from the injected noise. The heading, the road heading and the curvature are known exactly, and the only measurement error is σ_{gps} on the cross-track term. Constructing the lateral estimate is the principal difficulty in a real lane-keeping system, and that difficulty is absent here.

One flat lane. There is no camber, no superelevation, no width variation, no other traffic and no road grade, and the reference path is the exact centerline rather than something a perception system had to infer.

One first-order actuator. Real electric power steering adds compliance, friction and a torque limit that varies with speed, and the assist map is itself a function of vehicle speed. The model keeps one lag, one rate limit and one end stop, which is enough to produce the three distinct failure modes of Section 2.6 and no more.

2.4 Dynamic Analysis

2.4.1 Steering Law and Ideal Closed-Loop Response

The Stanley law adds three terms, as shown in Equation (2.7).

$$\delta_{law} = \underbrace{\psi_e}_{\text{heading}} + \underbrace{\arctan\left(\frac{k_e\,\hat{e}_{ct}}{v + k_{soft}}\right)}_{\text{cross-track}} + \underbrace{\arctan(L\kappa)}_{\text{feedforward}} \tag{2.7}$$

where k_e is the cross-track gain and k_{soft} keeps the argument finite as v goes to zero. The argument of the arctangent is dimensionless, because k_e carries units of inverse seconds and $\hat{e}_{ct}/(v + k_{soft})$ carries seconds. Neither feedback term regulates the lane position alone. The heading term drives ψ_e to zero, which leaves the vehicle traveling parallel to the lane at whatever offset it holds. The cross-track term must first build a heading error before the vehicle moves laterally and has no mechanism for removing that heading error afterward, so it overshoots and oscillates.

Linearizing Equation (2.1) and Equation (2.4) about a straight road for small angles, with $\psi_r = 0$ so that $\psi_e = -\psi$, gives the pair in Equation (2.8).

$$\dot{e}_{ct} = -v(\delta - \psi_e), \qquad \dot{\psi}_e = -\frac{v}{L}\delta \tag{2.8}$$

Substituting Equation (2.7) with $\kappa = 0$ and an instantaneous actuator, and writing $k' = k_e/(v + k_{soft})$ for the linearized cross-track slope, the heading term cancels identically and what remains is Equation (2.9).

$$\dot{e}_{ct} = -k' v\, e_{ct} = -\frac{k_e\, v}{v + k_{soft}}\, e_{ct} \tag{2.9}$$

The cross-track error decays as a first order lag with time constant $(v + k_{soft})/(k_e v)$, which is 0.917 s at 10 m/s and 0.861 s at 30 m/s for the default $k_e = 1.2/\text{s}$ and $k_{soft} = 1.0\,\text{m/s}$. A threefold change in speed moves the closed-loop time constant by 6 %, and the whole of that 6 % is the softening constant. With $k_{soft} = 0$ the time constant is exactly $1/k_e$ at every speed.

Pause. Try Exercise 2.1 before reading on.

Eliminating δ from Equation (2.8) rather than substituting gives the full ideal characteristic polynomial $(s + k_e^*)(s + v/L)$ with $k_e^* = k_e v/(v + k_{soft})$. The loop has two real poles and only one of them is speed-invariant. The cross-track pole is at $-k_e^*$, close to $-1.2/\text{s}$ at every highway speed, and the heading pole is at $-v/L$, which is –3.45/s at 10 m/s and –10.34/s at 30 m/s. The heading mode is the faster of the two and it accelerates with speed, which is the reason the two-term law produces no overshoot. The time-scale separation between the two modes widens as the speed rises, because speed multiplies the term that removes the heading error at the same time as it is divided out of the term that creates it. The law of Equation (1.7) commands a turn rate through a separate heading gain k_h, and both of its poles are free of speed. The car's law commands a steering angle with a unit heading term, so its heading pole is $-v/L$ and moves with speed, while the cross-track pole stays put in both.

2.4.2 Effect of the Arctangent on Loop Gain

The exact cancellation lives in the cross-track term alone. Because $\tan(\arctan x) = x$, the yaw rate that term produces is $(v/L) \cdot k_e e_{ct}/(v + k_{soft})$, which tends to $k_e e_{ct}/L$ as v grows past k_{soft} with no small-angle approximation anywhere. Both halves of that statement are plotted in Figure 2.2. The correction the law asks for at the lane edge, $e_{ct} = 1.75\,\text{m}$, is 19.29° at 5 m/s and 3.88° at 30 m/s, a factor of five across a factor of six in speed, while the yaw rates those two corrections produce differ by only 16 %.

The arctangent is commonly described as providing large-error saturation, and for this application that description requires qualification. At 25 m/s the argument reaches unity, where the arctangent first departs appreciably from its tangent line, only at $e_{ct} = (v + k_{soft})/k_e = 21.7\,\text{m}$. Inside the lane the argument is at most 0.081 and the arctangent returns 99.8 % of the linear value, so at highway speed the term acts as a proportional gain. The saturation is significant at low speed, where the same crossover error falls to 2.5 m at 2 m/s, and after a large excursion, where it bounds the commanded angle by 90° rather than allowing a large error to demand an angle with no physical meaning.

2.4.3 Curvature Feedforward and the Heading Reference Point

Holding a corner of radius R requires a sustained steering angle $\arctan(L/R)$, and Equation (2.10) confirms that this angle turns the vehicle at exactly the rate the road turns.

$$\delta_{ff} = \arctan(L\kappa) \implies \dot{\psi} = \frac{v}{L}\tan\delta_{ff} = v\kappa \tag{2.10}$$

The demand is set by the reference rather than by a load, and with the feedforward switched off the angle is produced only by allowing a cross-track error to grow until the arctangent term supplies it. In steady cornering the vehicle travels on a circle concentric with the path, so its heading is parallel

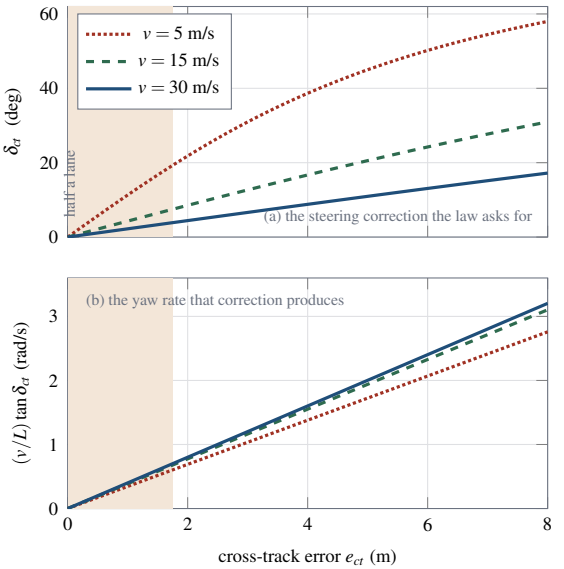


Figure 2.2 Speed entering the loop twice, at $k_e = 1.2/\text{s}$ and $k_{soft} = 1.0\,\text{m/s}$. The correction term $\delta_{ct} = \arctan(k_e e_{ct}/(v + k_{soft}))$ falls with speed while the yaw rate it produces does not, and the shaded strip is half a lane width. The dotted line is $v = 5\,\text{m/s}$, the dashed line 15 m/s and the solid line 30 m/s.

to the road heading beneath it and $\psi_e = 0$. Equating the remaining term to the required angle gives the standing offset of Equation (2.11).

$$e_{ct} = \frac{(v + k_{soft})\,L\,\kappa}{k_e} = \frac{(v + k_{soft})\,L}{k_e R} \tag{2.11}$$

For the shipped constant-radius configuration, $v = 25\,\text{m/s}$, $k_{soft} = 1.0\,\text{m/s}$, $L = 2.9\,\text{m}$, $k_e = 1.2/\text{s}$ and $R = 200\,\text{m}$, the prediction is 0.314 m and the measured steady error inside the corner is 0.314 m, on the outside of the bend. This is the classic proportional-offset argument of a controller without reset action [1], arriving from the reference rather than from a disturbance. Equation (1.8) is its counterpart for the turn-rate law of Chapter 1.

The same algebra determines why the heading error is referenced to the road under the vehicle. Taking it instead against the road direction at the front-axle projection adds $L\kappa$ to ψ_e, because the road heading advances by κ per unit of arc length and the two projections are approximately L apart. The heading term then already contains the feedforward, the vehicle body assumes an attitude offset of $\arctan(L\kappa)$ with the front wheel aligned on the path, and adding $\arctan(L\kappa)$ on top applies the same correction twice. Substituting that variant into the same steady-state balance predicts an offset of $-(v + k_{soft})L\kappa/k_e$, equal in size and opposite in sign. Running the simulator with the heading reference moved to the front-axle projection and the feedforward left on gives –0.3142 m in the same corner where the implemented pairing gives 0.000 m. A feedforward term is additive only when the equivalent term is not already implicit in the feedback path.

🕮 **Pause.** Try Exercise 2.2 before reading on.

2.4.4 Steady-State Offset Without Integral Action

The steering law contains no integral state, so any sustained demand that the feedforward does not supply leaves a standing error. A steering misalignment is the clearest case. The plant delivers

$\delta + \delta_{bias}$, so holding a straight line requires the law to produce $\delta = -\delta_{bias}$, and with $\psi_e = 0$ the offset is given by Equation (2.12).

$$e_{ct} = -\frac{(v + k_{soft}) \tan \delta_{bias}}{k_e} \tag{2.12}$$

At $\delta_{bias} = 0.6°$, $v = 25\,\mathrm{m/s}$ and $k_e = 1.2/\mathrm{s}$ the prediction is −0.227 m and the measured settled value is −0.227 m. Raising k_e to 2.6 reduces it to −0.105 m, and raising the misalignment to 2.0° increases it to −0.757 m. The offset falls as $1/k_e$ and never reaches zero, which is the consequence of a purely proportional geometric law and the reason Section 2.6 treats gain as a trade-off rather than as a free improvement.

2.4.5 Stability Limit Imposed by Actuator Lag

Restoring the actuator lag of Equation (2.2) to the linearized loop of Equation (2.8) turns the second-order characteristic polynomial into the cubic of Equation (2.13).

$$\tau_\delta s^3 + s^2 + \left(\frac{v}{L} + k_e^*\right) s + \frac{k_e^* v}{L} = 0 \tag{2.13}$$

The Routh condition for this cubic is $v/L + k_e^* > \tau_\delta k_e^* v/L$, which is satisfied for every positive gain whenever $\tau_\delta v < L$. At the default rack lag of 0.10 s that inequality holds for all $v < L/\tau_\delta = 29\,\mathrm{m/s}$, so across almost the whole speed range the application allows there is no cross-track gain that destabilizes the linearized loop. Above that speed, and at any speed once the rack is slowed down, the critical gain is finite and given by Equation (2.14).

$$k_{e,crit}^* = \frac{v/L}{\tau_\delta v/L - 1}, \qquad \omega_{crit} = \sqrt{\frac{k_{e,crit}^* v}{L}} \tag{2.14}$$

For the slow-rack configuration, $\tau_\delta = 0.45\,\mathrm{s}$ at 25 m/s, Equation (2.14) gives $k_{e,crit}^* = 2.99$, which corresponds to an entered gain of $k_e = 3.11$ after the k_{soft} correction, and an oscillation period of 1.24 s. A model run outside the settings the application offers, on the straight road and started from a 10 µm displacement so that no limit is active, loses small-signal stability between $k_e = 2.55$ and $k_e = 2.6$ with a measured period of 1.28 s. The 16 % gap is attributable to the sampled-data hold. Reducing the control period from 20 ms to 5 ms in the same run moves the measured boundary to between 2.95 and 3.0, and reducing it to 1 ms moves it to between 3.05 and 3.1, within 1 % of the continuous-time prediction. Tuning this loop at 50 Hz is therefore not tuning the plant of Equation (2.13), and the difference amounts to 0.5/s of gain margin. Sampled measurement and zero-order hold are ordinary features of a digital control loop [1, 4], and this configuration quantifies their cost on a loop whose continuous-time boundary is known in closed form.

2.5 Controller Design

2.5.1 Discrete Steering Algorithm

Under the Stanley law the steering path is a static function of geometry followed by two limits, and it runs to completion every $\Delta t_c = 0.02\,\mathrm{s}$ in both manual and automatic operation. The sequence is

1. project the front axle and read e_{ct} and κ at s^*,
2. project the rear axle and read ψ_r at s, form $\psi_e = \mathrm{wrap}(\psi_r - \psi)$,
3. form $\hat{e}_{ct}$ from Equation (2.5),
4. advance the speed setpoint, $v_{SP} \leftarrow \mathrm{clamp}(v_{SP} + \dot{v}_{SP}\Delta t_c, 2, 40)$,
5. form $\delta_{ff} = \arctan(L\kappa)$ if the feedforward is on and zero otherwise,

6. evaluate Equation (2.7) and clip the result to $\pm\pi/2$ for reporting,
7. select the request, $r = \delta_{law}$ when the steering loop is in automatic and $r = \delta_{man}$ otherwise,
8. clamp, $\delta_c = \mathrm{clamp}(r, -\delta_{max}, \delta_{max})$,
9. rate limit, $\delta_{cmd} \leftarrow \delta_{cmd} + \mathrm{clamp}(\delta_c - \delta_{cmd}, \pm\dot{\delta}_{max}\Delta t_c)$.

The saturation flag is raised when $|\delta_c| \geq \delta_{max}$ and the rate-limit flag when δ_{cmd} differs from δ_c after step nine, so the two failure modes are counted separately in the reported metrics. The clip to $\pm\pi/2$ in step six alters nothing the vehicle experiences, because step eight clamps to $\delta_{max} \leq 30^\circ$ in any case, and it bounds the reported law output for display.

2.5.2 Velocity Form Speed Loop

The longitudinal controller is the velocity-form PID of Section 1.6.2 [2], with the derivative taken on the measurement. In the loop's own symbols the error and the three increments are given by Equations (2.15) and (2.16).

$$
\begin{aligned}
e_{v,k} &= v_{SP,k} - v_k \\
\Delta u_k^P &= K_c \left(e_{v,k} - e_{v,k-1} \right) \\
\Delta u_k^I &= \frac{K_c}{\tau_I} e_{v,k} \Delta t_c \\
\Delta u_k^D &= -K_c \tau_D \frac{v_k - 2v_{k-1} + v_{k-2}}{\Delta t_c}
\end{aligned}
\tag{2.15, 2.16}
$$

where K_c is in 1/s, τ_I and τ_D are in seconds and Δt_c is the control period. The speed loop runs with $\tau_D = 0$, so Δu_k^D vanishes and the loop is proportional-integral. The increments are combined and the demand is clipped to the traction and braking envelope, as shown in Equation (2.17).

$$
\begin{aligned}
z_k &= z_{k-1} + \Delta u_k^P + \Delta u_k^D \\
c_k &= z_k + I_{k-1} \\
a_{cmd,k} &= \mathrm{clamp}\left(c_k,\ a_{min},\ a_{max} \right) \\
I_k &= I_{k-1} + \Delta u_k^I + \frac{\Delta t_c}{\tau_t} \left(a_{cmd,k} - c_k \right)
\end{aligned}
\tag{2.17}
$$

Here z_k accumulates the proportional and derivative increments without limit, c_k is the acceleration the algorithm demands, built on the integral accumulated through the previous scan, and $a_{cmd,k}$ is that demand clipped to the envelope. These are Equations (1.20) to (1.22), with z_k in place of S_k because s is the road station here. Anti-windup is back-calculation with a tracking time $\tau_t = \tau_I = 4\,\mathrm{s}$. There is no bias and no output rate limit, and the plant applies the same envelope the controller clips to. The plant $\dot{v} = a$ is a pure integrator, so proportional action alone already produces zero offset against a constant setpoint, and the integral term is required only on a ramp. In manual operation the pedal is mapped to acceleration by $a = (\mathrm{pedal}/100)\, a_{max}$ for a positive pedal and $a = -(\mathrm{pedal}/100)\, a_{min}$ for a negative one, and I_k is set each scan to the value that makes $z_k + I_k$ equal the operator-set acceleration, so transfer in either direction is bumpless with no additional logic (Section 1.6.2).

2.5.3 Bumpless Transfer of the Steering Loop

The steering law contains no integral state to seed, so continuity across a mode change comes from the rate limit of step nine instead. The command δ_{cmd} is carried across the mode switch and can leave the operator's last value only at $\dot{\delta}_{max}$, which is 45 °/s by default and therefore 0.9° in the first control interval. The law is evaluated and logged in manual operation as well, so the value the loop would command is available before the transfer occurs.

2.5.4 Manual Operation

The application opens with the steering loop in manual on a straight highway at 25 m/s and the road wheels centered. Incremental manual steering is bounded by a constant lateral acceleration envelope, $\min(\delta_{max}, \arctan(La_{lat}/\max(v^2,4)))$ with $a_{lat} = 5.0\,\mathrm{m/s^2}$, which is 1.33° at 25 m/s and 8.25° at 10 m/s, while the direct manual entry reaches the mechanical lock at any speed. The envelope is imposed because full lock at highway speed places the vehicle outside the lane within one second, which leaves no usable range for manual regulation.

Manual operation quantifies the scale of the problem. A steady 1° of steering at 25 m/s bends the path to a radius of $L/\tan 1^\circ = 166\,\mathrm{m}$, and the simulated vehicle, with its rack lag included, moves 1.53 m laterally in the first second after the command reaches the rack and 3.68 m in the first second and a half, against a half lane of 1.75 m. Manual corrections in the logged traces are whole degrees while the controller acts in tenths of a degree, because a manual correction responds to the visible position while the law responds to the position and the heading together.

2.5.5 Model Predictive Steering

A model predictive controller (MPC) is offered as a second steering law, and only configuration 11 selects it. The predictive option of the apps in general is described in Section 1.6.3. This app builds its own model, objective and estimator for the steering, set out below. It replaces δ_{law} in step seven and leaves the clamp, the rate limit and the speed loop as they are. Every 0.1 s it optimizes the steering over the coming $T_p = 2\,\mathrm{s}$, keeps only the opening move and repeats from the newest measurement, a receding-horizon scheme whose constrained form is reviewed in [18]. MPC of front steering on a vehicle model linearized afresh at each sample has been tested at up to 21 m/s on ice [19]. The Stanley law corrects the geometry of Figure 2.1 at the present instant. The MPC plans on that geometry, with the road ahead as a known preview and the steering offset as an estimated disturbance.

The controller's model is not identified. It is Equations (2.1), (2.2) and (2.4) written along the road for small angles, with the rack lag, a ramped command and a constant steering offset d, as shown in Equation (2.18).

$$\begin{gathered} \dot{e}_{ct} = v(\psi_e + \Delta\theta) - v(\delta + d), \qquad \dot{\psi}_e = v\kappa_r - \frac{v}{L}(\delta + d), \\ \tau_{\delta 0}\,\dot{\delta} = u - \delta, \qquad \dot{u} = \rho, \qquad \dot{d} = 0 \end{gathered} \tag{2.18}$$

Here u is the planned command, ρ its rate, d the angle by which the wheels turn past the command, playing the part of δ_{bias}, which the controller never reads, κ_r the curvature at the rear-axle projection and $\Delta\theta = \psi_r(s^*) - \psi_r(s)$ the road heading difference between the two projections, close to $L\kappa$ on an arc. The model is rebuilt and discretized at every decision at the measured speed v. The wheelbase L is read where the feedforward $\arctan(L\kappa)$ reads it, so a changed wheelbase reaches both laws, while $\tau_{\delta 0} = 0.10\,\mathrm{s}$ is the declared rack lag of Table 2.3, which the Stanley law never reads, so a slower rack is an error in the MPC's model alone. Stepped open loop on the commands of runs steered by the Stanley law, with the true offset as d, it errs two seconds ahead by 2.0 mm on configuration 11, 20.7 mm at 6.6° of steering on the $R = 25\,\mathrm{m}$ corner and 2.14 m on the 0.45 s rack of configuration 9.

A zero-order hold over the decision period $T_s = 0.1\,\mathrm{s}$, every fifth control period, gives $N = T_p/T_s = 20$ steps. The decisions are command rates held over nine move blocks, four single steps followed by blocks of 2, 2, 3, 4 and 5. The command therefore ramps in straight segments that the rate limiter passes unchanged, and each control period requests the mean of the first ramp over that period. The objective is Equation (2.19).

$$\begin{aligned} J = \sum_{k=1}^{N-1} \left[\frac{e_k^2}{s_e^2} + \frac{(\psi_k - \psi_k^*)^2}{s_\psi^2} \right] + \lambda \sum_{k=0}^{N-1} \frac{\rho_k^2}{s_\rho^2} \\ + \tilde{z}_N^T P \tilde{z}_N + q_\varepsilon \varepsilon^2 + r_\varepsilon \varepsilon \end{aligned} \tag{2.19}$$

Here e_k and ψ_k are the predicted errors, $\psi_k^* = L\kappa_{r,k} - \Delta\theta_k$ is the heading error that keeps e_{ct} at zero on the road of step k, $s_e = 0.1\,\text{m}$, $s_\psi = 1^\circ$, $s_\rho = 10^\circ/\text{s}$ and $\lambda = 0.01$. The vector $\tilde{z}_N$ is the departure of $(e_{ct}, \psi_e, \delta, u)$ from the rest state of the last step's road and the estimated offset, and P is the stationary Riccati solution with these weights, so the terminal term prices everything after the horizon as the linear quadratic regulator (LQR) would. When no constraint is active and each step carries its own decision, the opening rate of the plan matches the LQR's to 9.5×10^{-9} rad/s, on moves of up to 0.96 rad/s, against an independent construction. The weight λ was chosen once, on configuration 11, as the largest of twelve values within 10 % of the best lane IAE summed over both speeds, among those that kept the lane, rejected no plan and added at most 5 % to the Stanley law's steering travel.

The limits $|\rho_k| \le \dot{\delta}_{max}$ and $|u| \le \delta_{max}$, the angle bound imposed where each block ends and so holding for the whole ramp, are hard and are read as the clamp and the rate limiter read them. The lane is soft, $|e_k| \le w/2 - w_{car}/2 + \varepsilon$ with $\varepsilon \ge 0$, the 0.82 m margin of Equation (2.6) at the defaults, priced at $q_\varepsilon = 10^4$ per m^2 and $r_\varepsilon = 10^3$ per meter. Each plan is a quadratic program in the nine rates and the slack, with 77 inequality rows and a ridge of $10^{-9}(1 + 2\lambda N/s_\rho^2)$, which the dual active-set solver the apps share completes in one iteration on configuration 11 and in 7.5 on average, 36 at most, on configuration 8.

A steady-state Kalman filter on $(e_{ct}, \psi_e, \delta, d)$ at Δt_c, driven by the applied command and by $\Delta\theta$ and κ_r under the vehicle now, supplies the state each plan starts from. It is corrected by the two quantities the Stanley law measures, $\hat{e}_{ct}$ and ψ_e, with variances $(0.1\,\text{m})^2$ and $(0.01^\circ)^2$, against process variances per period of $(1\,\text{mm})^2$, $(0.057^\circ)^2$, $(0.181^\circ)^2$ and $(0.0057^\circ)^2$. Its gain is designed once at 25 m/s with the declared wheelbase and rack lag, and its transition matrix follows the measured speed. The estimate of d settles with a time constant of 2.95 s at 30 m/s and 5.27 s at 10 m/s, and the cross-track channel with 0.64 s. Carrying d as an integrating state lets the plan cancel a constant misalignment without offset [20], the same construction as the offset-free MPC of Volume 9, Chapter 4, whose estimator carries a fuel bias. The filter runs under both laws, so a switch to the MPC starts from a converged estimate.

With the preview on, the default, the plan reads $\Delta\theta_k$ and $\kappa_{r,k}$ from the road table the controller follows, at the stations the two axles reach at the measured speed. With it off the plan holds the front-axle curvature now, the number the feedforward reads, while the filter still reads the road under both axles, so the MPC is not reduced to the information of the Stanley law.

A plan is rejected when its program is not optimal, when its first rate is not finite or exceeds $\dot{\delta}_{max}$, or when its first block ends beyond δ_{max}. The Stanley law, evaluated in every period, then supplies the request through the rate limiter until a plan is accepted. Rejections forced at six instants of configuration 11 move the command by at most 0.58° in one period at the hand-over and 0.80° at the hand-back, inside the 0.90° limiter step, and no shipped configuration rejects a plan. The plant remains Equations (2.1) to (2.6) with the rack lag and misalignment of the run, behind the instrument of Equation (2.5), while the controller reads $\hat{e}_{ct}$, ψ_e, v, the road table and the limits. A decision, which rebuilds the model, solves the Riccati equation and solves the program, takes 0.18 to 0.29 ms on average in Node.js and 0.30 to 0.44 ms in Chrome, at most 1.7 % of a core at five times real time.

2.6 Results

Table 2.4 lists the shipped configurations, the app's numbered scenarios (Section 1.6.4), and the mechanism each one isolates. Each configuration fixes the road it requires and whatever else its lesson depends on and leaves every other setting at the default, so the change under test is always identifiable. Every number in Table 2.5 comes from the performance metrics the application computes while it runs, over a horizon of 40 s, which is long enough for each road to deliver all of its curvature, or 20 s for the offset start and 34 s for the challenge, the time at which its target is judged. Figure 2.3 draws the peak error of every configuration as a bar.

Table 2.4 Shipped Configurations and the Mechanism Each Isolates

Configuration	What it changes and what it shows
1 Straight highway	Manual, 25 m/s. Manual regulation followed by transfer to automatic while running.
2 Constant radius	$R = 200$ m at 25 m/s. Feedforward on against off, and Equation (2.11).
3 S-curve	$R = \pm 150$ m with clothoids. The error appears in the transitions rather than in the constant-curvature corners.
4 Lane change	3.5 m over 60 m. A steering-rate demand that scales with speed.
5 Speed ramp	10 to 30.4 m/s on one sweep with one tuning. The speed cancellation.
6 Sudden curvature	κ steps to $1/120$ with no spiral at 20 m/s. An actuator deficit that no gain removes.
7 Offset start	Starts 1 m right on a straight. First-order recovery at $1/k_e^*$.
8 Steering limit	$R = 25$ m at 10 m/s, $\delta_{max} = 6^\circ$, $k_e = 2.0$. Geometric infeasibility.
9 Slow rack	$\tau_\delta = 0.45$ s on the S-curve. Phase lag and the resulting gain limit.
10 Noisy measurement	$\sigma_{gps} = 0.25$ m on the gentle sweep. Actuator travel against tracking error.
11 MPC at two speeds	Lane change at 30 m/s with 0.5° of misalignment under the MPC, then the Stanley law, then both at 10 m/s. One gain against a model rebuilt at the measured speed.
12 Challenge	Challenge course at 20 m/s with 0.6° of misalignment and 0.07 m of noise, starting from $k_e = 0.5$, $k_{soft} = 4.0$, feedforward off.

Table 2.5 Measured Performance for Every Configuration Over a Fixed Horizon

Configuration	IAE (m s)	max $\lvert e_{ct} \rvert$ (m)	TV(δ) (rad)	sat (%)	out (%)
2 Constant radius, ff on	0.028	0.016	0.04	0.0	0.0
2 Constant radius, ff off	8.797	0.314	0.05	0.0	0.0
3 S-curve	0.124	0.014	0.11	0.0	0.0
3 S-curve, $k_e = 3$	0.050	0.007	0.11	0.0	0.0
4 Lane change, 25 m/s	0.073	0.023	0.15	0.0	0.0
4 Lane change, 12 m/s	0.029	0.004	0.14	0.0	0.0
5 Speed ramp	0.017	0.005	0.02	0.0	0.0
6 Sudden curvature	0.054	0.014	0.11	0.0	0.0
7 Offset start	0.866	1.000	0.07	0.0	1.7
8 Steering limit, $k_e = 2$	19.03	3.096	0.79	28.3	21.8
8 Steering limit, $k_e = 6$	21.20	3.074	1.58	41.4	26.9
8 Steering limit, $k_e = 12$	27.31	3.057	3.54	61.2	35.1
9 Slow rack, $k_e = 1.2$	0.969	0.126	0.17	0.0	0.0
9 Slow rack, $k_e = 3$	3.014	0.456	1.48	0.0	0.0
10 Noisy, $k_e = 1.2$	3.798	0.300	2.13	0.0	0.0
10 Noisy, $k_e = 4$	119.4	27.43	13.51	22.2	26.3
11 MPC, 30 m/s, as loaded	0.326	0.090	0.17	0.0	0.0
11 Stanley, 30 m/s	8.850	0.257	0.17	0.0	0.0
12 Challenge, as loaded	23.14	1.354	0.25	0.0	35.1
12 Challenge, tuned	3.095	0.214	1.27	0.0	0.0

Horizon 40 s except configuration 7 (20 s) and the challenge (34 s). The 12 m/s lane change starts at that speed, because the vehicle is initialized at the speed setpoint. IAE is the integrated absolute cross-track error, max $\lvert e_{ct} \rvert$ is the peak true error, TV(δ) is the total variation of the road-wheel angle in radians accumulated at the 20 Hz logging rate, sat is the fraction of the run with the steering request against its end stop, and out is the fraction with any part of the vehicle outside the lane markings.

2.6.1 Curvature as a Reference Demand

The constant-radius corner separates feedforward action from feedback action with no other effect present. With the feedforward on, the corner costs 0.016 m of peak error and 0.04 of steering travel, and the steering angle holds the geometric value $\arctan(L/R) = 0.831^\circ$ for the whole 28 s of the

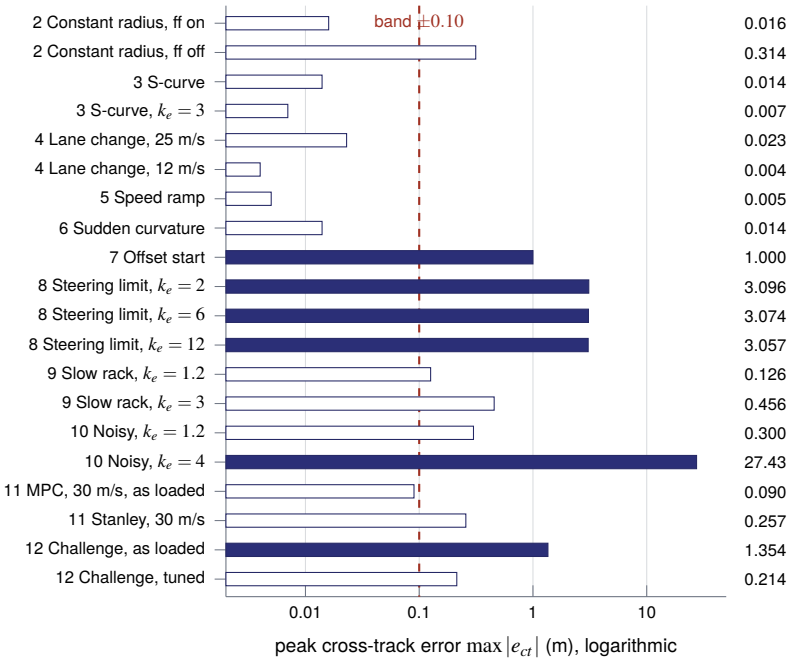


Figure 2.3 The peak cross-track error of Table 2.5, configuration by configuration, on a logarithmic axis, against the band of ±0.10 m (dashed line). Solid bars are runs with some time out of the lane, white bars runs that stayed in it. Notice that the corner the steering cannot reach keeps its peak near 3 m at every gain, that the missing feedforward and the misalignment under the Stanley law leave white bars past the band, and that the noisy road at $k_e = 4$ ends farthest from the lane.

arc. With the feedforward off, the same corner costs 0.314 m of standing error, and the integrated absolute error rises from 0.028 to 8.797, a factor of 317. The steering travel is nearly unchanged at 0.05, because the wheel reaches the same angle in both cases. The feedforward delivers the whole of that error reduction at no cost in actuator activity, which is the argument for supplying a known reference demand directly rather than requiring the feedback loop to develop an error large enough to produce it [1]. Section 1.4.4 makes the same argument for the reference feedforward of a moving cart.

2.6.2 Displacement Recovery at Two Speeds

Figure 2.4 shows the speed-cancellation experiment. The vehicle runs the gentle sweep while its speed setpoint ramps from 10 m/s to 30.4 m/s at 1.2 m/s^2 between $t = 3$ s and 20 s, and a 0.5 m lateral displacement is applied twice, at $t = 6.0$ s with the vehicle at 13.0 m/s and at $t = 27.0$ s at 30.6 m/s, with k_e held at 1.2/s throughout. Evaluated at the 10 ms integration step, the two recoveries decay to $1/\mathrm{e}$ of their initial value in 0.84 s and 0.85 s, against the 0.90 s and 0.86 s that Equation (2.9) predicts at those two speeds, and to 10 % in 2.07 s and 1.98 s respectively. The steering angles that produce those two nearly identical recoveries differ. The peak road-wheel deviation from the angle the road already required is 1.55° at 13.0 m/s, where the vehicle is on the approach straight and the required angle is zero, and 0.60° at 30.6 m/s, where the vehicle is inside the $R = 500$ m arc holding 0.332°. That is a ratio of 2.6 against a speed ratio of 2.35. The regulated variable behaves identically at the two speeds while the actuator excursion behind it differs by a factor of 2.6.

The remainder of the speed ramp shows the same result with no disturbance applied. The cross-track error over the whole 10 to 30.4 m/s ramp never exceeds 0.005 m and the steering angle holds the constant geometric value $\arctan(L/R) = 0.332°$ demanded by the $R = 500$ m sweep, because



Figure 2.4 One tuning across a three-to-one speed change, shown at $t = 40$ s. The speed setpoint ramps from 10 to 30.4 m/s on the gentle sweep while k_e stays at 1.2/s, and a 0.5 m lateral displacement is applied at $t = 6.0$ s (13.0 m/s) and again at $t = 27.0$ s (30.6 m/s). The two cross-track recoveries have the same shape and the same duration while the steering deviations that produce them differ by a factor of 2.6. The crop keeps the plant view and the trends and cuts the header and the side panels. Callouts: (1) the badges of the lateral error, steering angle, speed and lateral acceleration, (2) the car on the sweep, (3) the two cross-track recoveries, (4) the two steering deviations behind them, (5) the speed ramp.

that angle is set by geometry and carries no speed dependence either. The lateral acceleration does change, reaching 1.85 m/s^2 in the $R = 500$ m arc at 30.4 m/s as v^2/R, and 1.94 m/s^2 while the speed loop overshoots to 31.2 m/s just after the ramp ends.

TRY IT IN THE APP **5 · Increasing Speed (10 → 30 m/s on One Road)**

Load the case and press run. Watch the Speed trend climb from 10 to about 30 m/s while the Cross-track error trend stays flat: over the whole ramp the error never exceeds 0.005 m. The Steering angle trend holds near 0.332°, the angle the 500 m sweep needs at any speed.

2.6.3 Actuator-Limited Responses

Three configurations separate three distinct actuator limitations, and none of the three is a tuning problem.

The sudden-curvature road steps κ from zero to $1/120\,\mathrm{m}$ with no transition spiral, so the feedforward asks for $\arctan(L\kappa) = 1.384°$ instantly and the rack answers with a first-order lag. The resulting peak error is 0.014 m and feedback cannot remove it, because the deficit is in the actuator rather than in the law. Highway geometry standards specify transition spirals so that this step does not occur, which is one of the few cases in which civil engineering design is set explicitly by an actuator rate limit.

The lane change is a curvature pulse rather than a step, and it loads the steering rate rather than the steering angle. The curvature profile $\kappa(s)$ is a property of the road and does not change with speed, so the steering angle profile $\arctan(L\kappa)$ is the same at every speed. What changes is the time available to traverse it. The same 60 m of road is 2.4 s at 25 m/s and 5.0 s at 12 m/s, so the peak steering rate rises from 1.28 °/s at the lower speed to 2.76 °/s at the higher, a factor of 2.2, while both remain far below the 45 °/s limit, which is never reached. The measured peak error is 0.023 m at 25 m/s against 0.004 m at 12 m/s, and the steering travel is 0.15 against 0.14 because the wheel visits the same angles in both cases.

The sharp corner is not a tuning problem. Holding $R = 25\,\mathrm{m}$ needs $\arctan(L/R) = 6.617°$ and the configuration limits the steering to 6°, so the required angle exceeds the available angle and no gain closes the gap. Raising k_e from 2 to 6 to 12 leaves the peak error at 3.096 m, 3.074 m and 3.057 m, an improvement of 1.3 % over a sixfold increase in gain, while the time against the end stop rises from 28.3 % to 61.2 %, the time out of the lane rises from 21.8 % to 35.1 % and the steering travel rises from 0.79 to 3.54. The corner is infeasible for the available steering authority, and distinguishing that condition from a badly tuned loop is the practical result the configuration provides.

Pause. Try Exercise 2.3 before reading on.

2.6.4 Actuator Lag and the Gain Limit

The slow-rack configuration puts $\tau_\delta = 0.45\,\mathrm{s}$ on the S-curve and leaves everything else alone. At $k_e = 1.2/\mathrm{s}$ the loop crosses over near 1.2 rad/s, where the lag contributes $\arctan(1.2 \times 0.45) = 28.4°$ of phase, and the peak error grows from 0.014 m with the standard rack to 0.126 m. Raising k_e to 3 moves the crossover to the frequency where the lag contributes 53.5°, the heading term arrives after the vehicle has already turned, and the peak error over the reporting horizon grows to 0.456 m while the steering travel rises from 0.17 to 1.48. That gain is above the small-signal boundary of Equation (2.14), so the run is unstable rather than merely degraded. The 40 s horizon does not reveal the instability, because the road delivers curvature until 30.7 s and the growth has barely begun. Continued to 80 s on the straight that follows the last corner, the same run leaves the lane at 44.7 s and its envelope grows to 109.8 m over the last 20 s, while the $k_e = 1.2/\mathrm{s}$ run settles to 0.000 m. Reporting a stability conclusion therefore requires a horizon longer than the excitation.

2.6.5 Measurement Noise and Actuator Travel

The noisy-measurement configuration is the case in which raising the gain degrades every reported measure, and its endpoint is not predicted by the linear analysis. Table 2.6 shows the sweep. Between $k_e = 1.2$ and $k_e = 3.8$ the degradation is monotone. The true tracking error grows rather than falls, because the loop cannot distinguish a real displacement from a receiver wander, and the steering

Table 2.6 Cross-Track Gain Against Steering Travel With $\sigma_{gps} = 0.25\,\text{m}$ on the Gentle Sweep

k_e (1/s)	IAE (m s)	max $\lvert e_{ct}\rvert$ (m)	TV(δ) (rad)	rate lim. (%)	max $\lvert\delta_{law}\rvert$ (deg)
1.2	3.798	0.300	2.13	0.0	1.9
2.0	4.918	0.435	3.73	2.5	3.2
3.0	5.878	0.549	5.99	17.7	5.3
3.5	6.326	0.589	7.41	29.7	6.5
3.8	6.781	0.726	8.54	38.35	8.8
4.0	119.4	27.43	13.51	53.3	90.0

travel grows fourfold while the fraction of the run spent against the rate limit rises from zero to 38.35 %.

At $k_e = 4.0$ the loop diverges. The peak error increases from 0.726 m to 27.43 m, the vehicle spends 26.3 % of the run outside the lane and 22.2 % of it against the steering end stop, and the law reaches its own 90° reporting clip. Equation (2.14) shows that this is not a linear instability, because $\tau_\delta v = 2.5\,\text{m}$ is smaller than $L = 2.9\,\text{m}$ at this speed and rack lag, and the same gain on the same road with the noise removed holds the line to 0.001 m. The cause is the rate limiter. The noise-driven command excursions grow with k_e until they demand more than 45 °/s, and a rate limiter that is active for half the run acts as an amplitude-dependent phase lag that no small-signal margin accounts for. The logged traces show the command trailing the law by several degrees for about a second before the first departure at 29.4 s, and at the departure the law requests −23.8° while the command is still passing through −1.6°. The location of the cliff depends on the noise sequence. The table uses the shipped sequence, and across eleven other seeds, on the same gains extended to 4.2 and 4.5, the first gain to leave the lane within 40 s ranges from 3.8 to 4.5, while no seed fails at 3.5.

Actuator travel is therefore read alongside the tracking error rather than the tracking error alone. A tuning that is acceptable on the cross-track record can be cycling the steering rack thousands of times an hour, which is a durability cost in the vehicle and a ride quality cost for the occupants, and it can be one increment of gain below a discontinuous loss of control.

> ✦ DID YOU KNOW? **One Step of Gain Past the Edge**
>
> From the simulator: on the gentle sweep with 0.25 m of measurement noise, a cross-track gain of 3.8 keeps the peak error at 0.726 m. A gain of 4.0 takes it to 27.43 m, with the command on its rate limit for 53.3 % of the run (Table 2.6). Without the noise the same gain holds the line to 0.001 m.

2.6.6 The Graded Challenge

The challenge configuration combines three mechanisms with conflicting gain requirements. The course is a left-hand corner running into a right-hand one at 20 m/s, the linkage is misaligned by 0.6°, the lateral measurement carries 0.07 m of noise, and the starting tuning is deliberately weak at $k_e = 0.5$, $k_{soft} = 4.0$ and the feedforward switched off. The target is judged after the 680 m course, at $t = 34\,\text{s}$. As loaded the configuration fails it, with a peak error of 1.354 m, 5.4 times the band, and 35.1 % of the run outside the lane, without reaching the steering limit. Equation (2.11) accounts for most of that on its own, predicting $24 \times 2.9/(0.5 \times 140) = 0.99\,\text{m}$ in the first corner, and Equation (2.12) adds a further 0.50 m from the misalignment. Enabling the feedforward removes the first contribution completely and at no cost in actuator travel. The second contribution falls as $1/k_e$ while the noise response grows with k_e, and the suggested setting of $k_e = 2.6$, $k_{soft} = 1.0$ with the feedforward on meets the $\pm 0.25\,\text{m}$ target with a peak of 0.214 m, no saturation and no departure, at the cost of raising the steering travel from 0.25 to 1.27. The same settings applied before a Reset give the same result. The 0.036 m margin belongs to the shipped noise sequence. Across eleven other seeds the same tuning peaks between 0.180 m and 0.255 m and exceeds the band on two of them.

Table 2.7 Stanley Law Against MPC With Configuration 11's Settings

Case	Law	max $\lvert e_{cr} \rvert$ (mm)	RMS (mm)	IAE (m s)	TV(δ) (rad)	ψ_e (deg)	rate (%)	sat (%)	out (%)
11, 30 m/s	Stanley	256.6	222.2	8.850	0.168	0.058	0	0	0
	MPC	89.5	20.3	0.326	0.169	0.058	0	0	0
	no prev.	89.5	20.3	0.327	0.181	0.059	0	0	0
11, 10 m/s	Stanley	85.7	78.7	3.136	0.148	0.078	0	0	0
	MPC	33.4	11.1	0.249	0.153	0.063	0	0	0
30 m/s, d 0	Stanley	34.1	6.8	0.090	0.151	0.014	0	0	0
	MPC	5.5	1.1	0.014	0.136	0.035	0	0	0
	no prev.	11.3	1.4	0.017	0.148	0.037	0	0	0
2	Stanley	15.5	2.3	0.028	0.036	0.021	0	0	0
	MPC	8.3	0.8	0.009	0.034	0.024	0	0	0
6	Stanley	14.4	3.1	0.054	0.114	0.060	0.05	0	0
	MPC	16.8	2.4	0.035	0.132	0.066	0	0	0
7	Stanley	1000.0	151.7	0.866	0.065	0.390	0.20	0	1.7
	MPC	1000.0	112.1	0.343	0.190	0.631	1.50	0	1.4
8	Stanley	3096.2	1009.1	19.03	0.790	3.449	0.90	28.3	21.8
	MPC	2605.2	797.5	14.28	0.827	3.054	0.75	31.2	17.9
9	Stanley	125.7	41.8	0.969	0.175	0.127	0	0	0
	MPC	65.5	21.1	0.610	0.244	0.125	0	0	0
10	Stanley	299.9	115.1	3.798	2.127	0.591	0	0	0
	MPC	311.5	126.6	4.151	1.367	0.531	0	0	0
12	Stanley	213.9	104.9	3.095	1.266	0.371	0	0	0
	MPC	124.3	53.7	1.526	0.394	0.189	0	0	0

The first rows are configuration 11 with its 0.5° misalignment and without it (d 0). Stanley is the shipped tuning, $k_e = 2$ on configuration 8 and the suggested tuning on the challenge (12), and *no prev.* the MPC with the preview off. Peak and RMS are the true error at the 10 ms step, ψ_e the RMS heading error, rate the time on the rate limit. Every MPC run plans every 0.1 s and rejects no plan.

2.6.7 Stanley Law Against Model Predictive Steering

Table 2.7 compares the Stanley law, tuned as shipped, with the MPC run at the settings of configuration 11, with no retuning per case and the seeds, noise, instruments and horizons of Table 2.5. The feedforward reads the curvature at the front axle now, while the MPC reads 2 s of road ahead, which the rows marked *no prev.* withhold from its plan.

Configuration 11 drives the lane-change road at 30 m/s with the linkage misaligned by 0.5°, under each law and again at 10 m/s. Without integral action the Stanley law settles where Equation (2.12) puts it, 225.4 mm off the line at 30 m/s and 80.0 mm at 10 m/s, as measured at 20 and 40 s, so one gain resists the offset $31/11 = 2.82$ times less at the higher speed. The MPC's estimate of d is 0.244° at 2 s and 0.499° at 20 s, its error stays under 1 mm after 14.1 s, and its peak of 89.5 mm comes 0.25 s after the start, before the offset is known. Its lane IAE is 0.326 against 8.850 m s at 30 m/s and 0.249 against 3.136 m s at 10 m/s, for steering travel of 0.169 against 0.168 rad and 0.153 against 0.148 rad, as shown in Figure 2.5. At 20 s both laws hold the wheel at −0.500°, the Stanley law through a standing error and the MPC through its estimate.

Without the misalignment the same road separates the laws by less, peaks of 5.5 against 34.1 mm at 30 m/s and 3.0 against 5.8 mm at 10 m/s, which is why configuration 11 carries the offset. The Stanley law turns when the curvature reaches the front axle, and the rack lag then costs 3.0 m of road at 30 m/s, while the MPC turns before the shift arrives. With the preview off it still peaks at only 11.3 mm, but not on the Stanley law's information, because its filter reads the road heading at the front axle and the curvature under the rear axle. A counterfactual outside the application that gives the filter only the front-axle curvature as well peaks at 39.1 mm against 34.1 mm, while the misaligned case keeps its result (lane IAE 0.370 against 8.850 m s). The gain without the offset is therefore the road information's and the gain with it the estimator's. On these clean roads the MPC holds more heading error, 0.035° RMS against 0.014°, because its objective treats 0.1 m of cross-track error and 1° of heading error alike.

The MPC also lowers the peak on configurations 3, 4 and 5 (2.2, 4.0 and 0.6 against 13.8, 22.9 and

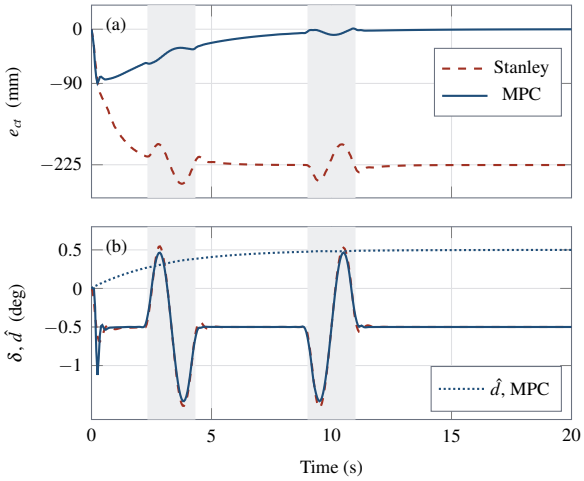


Figure 2.5 Configuration 11 at 30 m/s with 0.5° of misalignment under the MPC as loaded and under the Stanley law. (a) Cross-track error. (b) Road-wheel angle under both laws and the MPC's offset estimate $\hat{d}$ (dotted). The Stanley law is dashed and the MPC solid. Shading marks the two lane shifts.

4.7 mm). It loses the sudden curvature on peak, 16.8 against 14.4 mm, with a lower IAE but more travel. From the offset start it steers harder, with 1.50 % of the run on the rate limit against 0.20 % and heading errors up to 5.58° against 2.60°, because the vehicle starts 0.18 m past the priced lane band. On the steering limit it is out of the lane for 17.9 % of the run against 21.8 % but on the end stop for 31.2 % against 28.3 %, because its preview sees the infeasible corner and its command reaches 6° at 6.71 s against 7.17 s. On the noisy measurement it moves the steering less, 1.367 against 2.127 rad, and tracks less closely, a lane IAE of 4.151 against 3.798 m s, because the filter that estimates the offset also smooths the receiver noise. On the straight highway without noise or misalignment, a −1.5° heading kick at 30 m/s takes it to 133.5 against 118.3 mm, though it wins at 10 m/s (14.8 against 20.9 mm RMS over 8 s), and a 0.5 m displacement is recovered more slowly (147.3 against 124.8 mm RMS at 10 m/s, 127.2 against 117.4 mm at 30 m/s), because the filter admits a measured jump over 0.64 s where the Stanley law acts on it at once.

With the preview off the MPC loses both curvature steps, because a plan that holds the front-axle curvature assumes the whole vehicle is already on the new arc. On the constant radius it commands up to 2.62° where the arc needs 0.831° and peaks at 36.9 against 15.5 mm, and on the sudden curvature it commands 4.05° where 1.384° is needed and peaks at 55.2 against 14.4 mm, with 0.439 against 0.114 rad of travel.

The rack lag is the decisive limitation, because the plan and the filter keep the declared 0.10 s. On the 0.45 s rack of configuration 9 as loaded, at 25 m/s, the MPC halves the peak, 65.5 against 125.7 mm, with more travel, 0.244 against 0.175 rad, but is lightly damped. After a gust on the straight, its largest error over 50 to 70 s is 0.241 of that over 10 to 30 s, against 0.000 for the Stanley law, and bisection on that ratio reaching one puts the MPC's limit at 32.3 m/s on a 0.40 s rack, 26.4 m/s on 0.45 s, 22.2 m/s on 0.50 s and 16.9 m/s on 0.60 s, while the Stanley law at $k_e = 1.2/\mathrm{s}$ is stable to 35 m/s on all four, as Equation (2.14) predicts, because its critical gain exceeds $1/\tau_\delta \geq 1.67/\mathrm{s}$ at every speed. On the S-curve at 30 m/s the MPC's error reaches 40.3 m within 80 s, where the Stanley law peaks at 174 mm. More move suppression lowers the limit, from 27.7 m/s at $\lambda = 0.001$ to 20.4 m/s at $\lambda = 1$, and neither a 0.5 nor a 4 s horizon holds 35 m/s. Told the true rack, in a counterfactual outside the application, the MPC holds the same S-curve to 3.5, 5.1 and 6.9 mm at 25, 30 and 35 m/s, so the loss belongs to the declared actuator and not to the method.

For information, the challenge is met with only the steering law changed. The MPC peaks at 0.124 m, never reaches the end stop or the rate limit, never leaves the lane and moves the steering 0.394 rad against the 1.266 rad of the suggested tuning, over 340 plans with none rejected, and the run breaks no limit that the target leaves unscored. The challenge and its suggested answer are left as shipped.

2.6.8 Implementation

Manual and automatic operation are provided for the steering loop and the speed loop independently, and the road, the tuning, the disturbances and the parameters of Table 2.3 are operator-set inputs. Every logged column, including the true and measured cross-track errors, the law output, the command and the achieved steering angle, is in the exported file of Section 1.6.4.

2.7 Technology in Practice

The car of Section 2.3 measures one lateral offset and is moved by one rack. A real lane-keeping system reads the lane with a camera or a positioning receiver, steers through the power steering and answers to a steering regulation. Figure 2.6 draws the chapter's two loops with such devices in place.

What Measures It

A camera-based system takes the lateral offset from lane lines found in the front-view image and projected onto the ground [21]. A positioning receiver is the other route. On the robot that won the 2005 desert race, receivers on the roof and an inertial measurement unit formed the positioning group that estimated the location and velocity of the vehicle, and the wheel speeds and the steering angle reached its computers over the vehicle bus [9]. In this chapter only $\hat{e}_{ct}$ carries an error, colored noise with a correlation time of 0.35 s, and the heading, the curvature and the speed are exact.

> **TECHNOLOGY** **Sensor: Lane-Detecting Camera**
>
> A camera-based system reads the lane from the front-view image of an onboard camera. A detector finds each lane line in the image, and the camera's intrinsic and extrinsic parameters project those lines onto the ground. The projection assumes flat ground, so an uphill, a downhill or a rough surface gives wrong lane positions even when the detection in the image is right. Lanes may also be hidden by nearby vehicles or by adverse weather. A laser scanner measures depth directly and does not mind the lighting, but its shorter range and high cost have kept cameras the more common choice [21]. The chapter's one imperfect instrument, the colored noise σ_{gps} on $\hat{e}_{ct}$, stands in for such errors without modeling them.

What Moves It

On the desert robot a direct-current motor attached to the steering column provided the electronic steering control [9]. In a production car the steering control may also operate without direct action of the driver, when a driver assistance steering system acts through it [22], and the power steering motor does the work. The regulation bounds that authority from the driver's side, since the effort needed to override the system may not exceed 50 N [22]. The rack of Equation (2.2) stands for the motor, the gear and the linkage together.

> **TECHNOLOGY** **Final Element: Electric Power Steering**
>
> An electric power steering unit adds motor torque to the driver's. Its control unit computes the assist from the torque the driver applies, the steering wheel position and the vehicle speed, with more assist at low speed than at high speed, and the motor turns the steering gear. The motor may sit on the column, on the pinion or on the rack, and the rack form, with its high reduction ratio, suits mid-size to full-size vehicles. Current systems keep a mechanical link from the steering wheel to the gear, and a detected fault in the control unit disconnects power from the motor [23]. The chapter compresses the unit, the gear and the linkage into one lag of 0.10 s, a rate limit and an end stop.

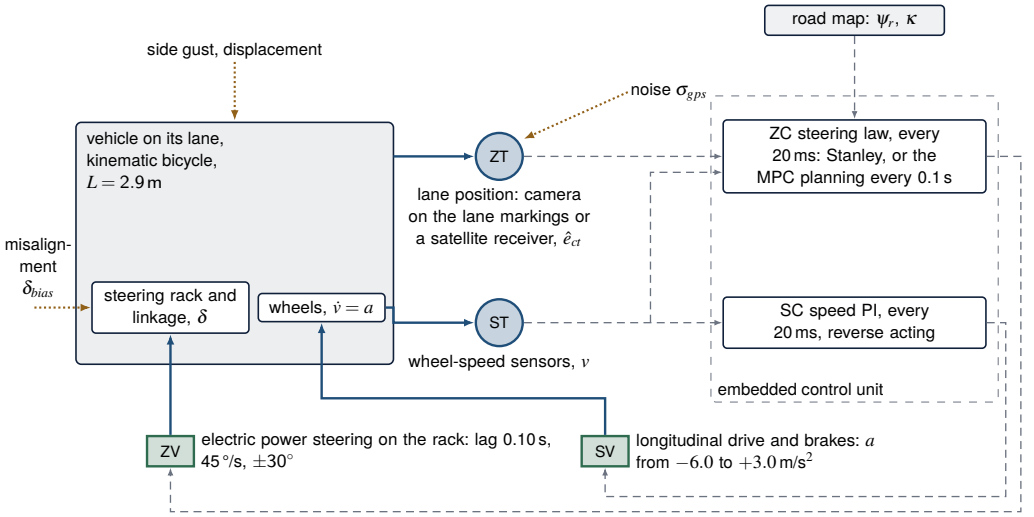


Figure 2.6 The lane loop and the speed loop of the chapter with real devices in place of the schematic's symbols. ZT reads the lane position, ST the wheel speeds, and one embedded control unit (dashed frame) runs the steering law (ZC) and the speed PI (SC) every 20 ms. ZV is the electric power steering on the rack, SV the drive and brakes. Notice that the misalignment enters at the linkage, after the actuator that reports the angle, so no sensor of the loop sees it, while the noise acts on the lane position alone.

Where the Controller Runs

The steering law runs on an embedded control unit in the vehicle. The desert robot's computers polled their sensors at up to 100 Hz and commanded the steering, throttle and brake at up to 20 Hz, the rate of its steering controller [9]. The chapter's controller runs at 50 Hz, a 20 ms period, and its predictive option plans every 0.1 s. The Stanley law is a static function block followed by a clamp and a rate limiter, and the speed loop is the velocity-form block of Section 1.6.2. Above both sits a supervisory layer that the model leaves out. The regulation asks a lane-keeping function to detect whether the driver holds the steering control, to warn after 15 s without hands and to switch itself off at the latest 30 s after its acoustic warning starts [22].

What Is Modernizing It

The first development is lane detection by deep learning on camera images, with networks that predict lanes in three dimensions directly rather than through a flat-ground projection [21]. The second is maps of the lanes estimated online from the vehicle's own sensors and computation, in place of maps built offline at a large cost in manual annotation [21]. The third is steer-by-wire, which removes the mechanical link from the steering wheel to the gear, and whose first production application kept a mechanical back-up [23]. The predictive steering of Section 2.5.5 belongs to the same move toward model-based control, and its loss on a slow rack shows what such a model must get right.

> ⚠ **IN PRACTICE** **What a Lane-Keeping Assist Must Meet**
>
> UN Regulation No. 79 on steering equipment names a function that assists the driver in keeping the vehicle within the chosen lane an automatically commanded steering function of Category B1. For passenger cars the lateral acceleration it is specified to hold may be at most 3 m/s^2, the half-second average of the lateral jerk it generates at most 5 m/s^3, and the driver must be able to override it with at most 50 N at the steering control. Type tests drive a curve at 80 to 90 % of the specified maximum [22]. The sharp corner of configuration 8 demands 4.0 m/s^2, beyond what such an assist may be specified to hold.

2.8 Limitations

The main limitation is the absence of tire forces. The results on geometry, feedforward and actuator limits are unaffected by the omission, and no result about the limit of adhesion can be obtained from this model. A real vehicle at $4\,\mathrm{m/s^2}$ of lateral acceleration generates measurable slip angles, the achieved curvature falls below $\tan\delta/L$, and the gap between the kinematic prediction and the dynamic one widens with speed in a way the Stanley division by v does not model [16]. Volume 7, Chapter 10 carries brush-model tires to the friction limit, where the kinematic picture no longer holds.

Localization is the second limitation and the larger one in practice. The heading, the road heading and the curvature are exact here, and the only imperfect quantity is the lateral offset. A camera-based system estimates all four from the same images with correlated errors, a latency of tens of milliseconds and a curvature estimate that degrades where the road curves most. The noise configuration in this application is therefore a stand-in rather than a model of a real perception chain. A moving horizon estimator built on Equations (2.1) to (2.5) would be the natural way to close that gap within the same model [24].

The steering actuator is one first-order lag with two hard limits. Real electric power steering has a torque limit rather than an angle-rate limit, and production lane-keeping systems bound that torque well below what the rack could deliver so that the driver can override the system at any time. Modeling the authority limit as an angle limit reproduces the saturation behavior but not the handover behavior, and the handover accounts for most of the human factors difficulty [11].

The predictive controller's model omits the actuator as it is. It carries the declared rack lag of 0.10 s, so on the 0.45 s rack of configuration 9 its prediction errs by 2.14 m two seconds ahead and its loop is unstable above 26.4 m/s, a loss the Stanley law, which carries no actuator model, does not suffer at any speed up to 35 m/s. The model also holds the speed over the horizon, linearizes the trigonometric terms and omits the clamp of $\delta + d$ at the end stop and the 20 ms staircase of the command, and the filter that removes the offset delays the answer to a measured jump.

Three smaller omissions are stated for completeness. The two loops do not compete for tire adhesion, so the vehicle can brake at $6\,\mathrm{m/s^2}$ while cornering at the same time. The road is a single lane with no camber, no superelevation and no other traffic. The projection is windowed and monotone, so it cannot jump to another pass of a road that doubles back, but it also cannot recover a vehicle placed far from its last station. The global nearest-point search that would do so is correct only where the road does not double back near the query point, and it appears only in the verification tests for that reason.

> ⚠ **OPEN CHALLENGE** **Seeing the Lane When the Paint Is Hidden**
>
> Both steering laws of this chapter assume a lane they can measure. A camera loses it where nearby vehicles or adverse weather obscure the markings, and a flat-ground projection misplaces it on slopes and rough roads. A recent survey finds notably few dedicated works on detection that pairs the camera with a laser scanner, which lighting does not affect [21]. The regulation concedes the gap: the lateral acceleration an assist is specified for may not be achievable in inclement weather, with different tires or on laterally sloped roads [22]. Progress would be lane estimates that state their own confidence, so that the controller can hand back to the driver before the measurement fails.

2.9 Conclusion

This chapter studied autonomous lane keeping on a five-state kinematic bicycle and a road stored as an arc-length table integrated from a curvature profile. The regulated variable is the cross-track error of the front axle and the heading error is referenced to the road under the vehicle, a pairing that keeps $\arctan(L\kappa)$ out of the feedback path so that the curvature feedforward supplies it once rather than twice. The default steering law is the Stanley construction with no integral action, followed by an end stop and a rate limit, over a velocity form proportional-integral speed loop. The ideal closed loop

carries poles at $-k_e v/(v+k_{soft})$ and $-v/L$, and the standing offsets left by a missing feedforward and by a misaligned linkage are confirmed to three decimal places against the running application.

Twelve configurations quantify the outcome, from a corner that costs 0.314 m without feedforward and 0.016 m with it, to a 25 m corner that no gain holds because 6.617° of steering is not available. One tuning holds a 0.5 m displacement recovery to 0.84 s and 0.85 s at 13.0 m/s and at 30.6 m/s while the steering deviation behind it changes by a factor of 2.6, and the effects the cancellation omits, a fixed actuator time spent covering a growing distance and a lateral acceleration rising as v^2, are what eventually limit it.

A model predictive controller removes the standing error of a 0.5° misalignment at 30 m/s (lane IAE 0.326 against 8.850 m s) but loses stability above 26.4 m/s on a 0.45 s rack that its 0.10 s model misjudges and the Stanley law holds. The same model supports extension to nonlinear model predictive control and to moving horizon estimation of the heading, the curvature and the steering misalignment. A fuller model would add a lateral tire model, a torque-limited rack with driver override and a comparison against pure pursuit on the same roads. The application makes measurable what a geometric path-following law does when the operating point moves beneath it.

KEY POINTS

- The steering law asks for less steering as the car goes faster, so one tuning recovers from a 0.5 m sideways displacement in 0.84 s at 13.0 m/s and 0.85 s at 30.6 m/s.
- Without integral action, a missing curvature feedforward leaves 0.314 m of standing error in the 200 m corner, and a misaligned linkage an offset that never reaches zero.
- A corner that needs 6.617° cannot be held with 6° of steering at any gain: an actuator limit, not a tuning problem.
- A predictive controller that estimates the misalignment removes its offset but loses stability above 26.4 m/s on a 0.45 s rack its model misjudges.

Where else this applies. Chapter 9 follows its routes by pure pursuit, and Volume 9, Chapter 4 removes an offset through an estimated bias, as the predictive steering here does.

References

[1] D. E. Seborg, T. F. Edgar, D. A. Mellichamp, and F. J. Doyle, III, *Process Dynamics and Control*, 4th ed. Hoboken, NJ: John Wiley & Sons, 2016.

[2] K. J. Åström and T. Hägglund, *Advanced PID Control*. Research Triangle Park, NC: ISA – The Instrumentation, Systems, and Automation Society, 2006.

[3] B. W. Bequette, *Process Control: Modeling, Design, and Simulation*. Upper Saddle River, NJ: Prentice Hall, 2003.

[4] K. J. Åström and R. M. Murray, *Feedback Systems: An Introduction for Scientists and Engineers*, 2nd ed. Princeton, NJ: Princeton University Press, 2021.

[5] J. B. Cicchino, "Effects of lane departure warning on police-reported crash rates," *Journal of Safety Research*, vol. 66, pp. 61–70, 2018.

[6] M. Rokonuzzaman, N. Mohajer, S. Nahavandi, and S. Mohamed, "Review and performance evaluation of path tracking controllers of autonomous vehicles," *IET Intelligent Transport Systems*, vol. 15, no. 5, pp. 646–670, 2021.

[7] E. D. Dickmanns and B. D. Mysliwetz, "Recursive 3-D road and relative ego-state recognition," *IEEE Transactions on Pattern Analysis and Machine Intelligence*, vol. 14, no. 2, pp. 199–213, 1992.

[8] C. Urmson, J. Anhalt, D. Bagnell, C. Baker, R. Bittner, M. N. Clark, J. Dolan, D. Duggins, T. Galatali, C. Geyer, M. Gittleman, S. Harbaugh, M. Hebert, T. M. Howard, S. Kolski, A. Kelly, M. Likhachev, M. McNaughton, N. Miller, K. Peterson, B. Pilnick, R. Rajkumar, P. Rybski, B. Salesky, Y.-W. Seo, S. Singh, J. Snider, A. Stentz, W. Whittaker, Z. Wolkowicki, J. Ziglar, H. Bae, T. Brown, D. Demitrish, B. Litkouhi, J. Nickolaou, V. Sadekar, W. Zhang, J. Struble, M. Taylor, M. Darms, and D. Ferguson, "Autonomous driving in urban environments: Boss and the Urban Challenge," *Journal of Field Robotics*, vol. 25, no. 8, pp. 425–466, 2008.

[9] S. Thrun, M. Montemerlo, H. Dahlkamp, D. Stavens, A. Aron, J. Diebel, P. Fong, J. Gale, M. Halpenny, G. Hoffmann, K. Lau, C. Oakley, M. Palatucci, V. Pratt, P. Stang, S. Strohband, C. Dupont, L.-E. Jendrossek, C. Koelen, C. Markey,

C. Rummel, J. van Niekerk, E. Jensen, P. Alessandrini, G. Bradski, B. Davies, S. Ettinger, A. Kaehler, A. Nefian, and P. Mahoney, "Stanley: The robot that won the DARPA Grand Challenge," *Journal of Field Robotics*, vol. 23, no. 9, pp. 661–692, 2006.

[10] G. M. Hoffmann, C. J. Tomlin, M. Montemerlo, and S. Thrun, "Autonomous automobile trajectory tracking for off-road driving: Controller design, experimental validation and racing," in *2007 American Control Conference*. IEEE, 2007, pp. 2296–2301.

[11] R. Parasuraman and V. Riley, "Humans and automation: Use, misuse, disuse, abuse," *Human Factors*, vol. 39, no. 2, pp. 230–253, 1997.

[12] A. Ollero and G. Heredia, "Stability analysis of mobile robot path tracking," in *Proceedings 1995 IEEE/RSJ International Conference on Intelligent Robots and Systems*, vol. 3. IEEE Computer Society Press, 1995, pp. 461–466.

[13] S. Macenski, S. Singh, F. Martín, and J. Ginés, "Regulated pure pursuit for robot path tracking," *Autonomous Robots*, vol. 47, no. 6, pp. 685–694, 2023.

[14] B. Paden, M. Čáp, S. Z. Yong, D. Yershov, and E. Frazzoli, "A survey of motion planning and control techniques for self-driving urban vehicles," *IEEE Transactions on Intelligent Vehicles*, vol. 1, no. 1, pp. 33–55, 2016.

[15] J. Kong, M. Pfeiffer, G. Schildbach, and F. Borrelli, "Kinematic and dynamic vehicle models for autonomous driving control design," in *2015 IEEE Intelligent Vehicles Symposium (IV)*. IEEE, 2015, pp. 1094–1099.

[16] P. Polack, F. Altché, B. d'Andréa Novel, and A. de La Fortelle, "The kinematic bicycle model: A consistent model for planning feasible trajectories for autonomous vehicles?" in *2017 IEEE Intelligent Vehicles Symposium (IV)*. IEEE, 2017, pp. 812–818.

[17] M. Guiggiani, *The Science of Vehicle Dynamics: Handling, Braking, and Ride of Road and Race Cars*. Cham: Springer, 2023.

[18] D. Q. Mayne, J. B. Rawlings, C. V. Rao, and P. O. M. Scokaert, "Constrained model predictive control: Stability and optimality," *Automatica*, vol. 36, no. 6, pp. 789–814, 2000.

[19] P. Falcone, F. Borrelli, J. Asgari, H. E. Tseng, and D. Hrovat, "Predictive active steering control for autonomous vehicle systems," *IEEE Transactions on Control Systems Technology*, vol. 15, no. 3, pp. 566–580, 2007.

[20] G. Pannocchia and J. B. Rawlings, "Disturbance models for offset-free model-predictive control," *AIChE Journal*, vol. 49, no. 2, pp. 426–437, 2003.

[21] X. He, H. Guo, K. Zhu, B. Zhu, X. Zhao, J. Fang, and J. Wang, "Monocular lane detection based on deep learning: A survey," arXiv:2411.16316v5, 2024.

[22] United Nations Economic Commission for Europe, "UN Regulation No 79 – Uniform provisions concerning the approval of vehicles with regard to steering equipment [2025/3]," Official Journal of the European Union, L series, 10 January 2025, http://data.europa.eu/eli/reg/2025/3/oj, 2025.

[23] Clemson Vehicular Electronics Laboratory, "Electric power-assisted steering," Clemson University, http://cecas.clemson.edu/cvel/auto/systems/ep_steering.html, accessed 2026-11-20, 2026.

[24] J. D. Hedengren, R. Asgharzadeh Shishavan, K. M. Powell, and T. F. Edgar, "Nonlinear modeling, estimation and predictive control in APMonitor," *Computers & Chemical Engineering*, vol. 70, pp. 133–148, 2014.

2.10 Exercises

2.1 ⌕ Concept check · 2 min

With the default tuning, $k_e = 1.2/\mathrm{s}$ and $k_{soft} = 1.0\,\mathrm{m/s}$, a cross-track error decays with nearly the same time constant at 10 m/s and at 30 m/s, although the yaw rate a given steering angle produces is three times larger at the higher speed. Why?

(a) The law divides the cross-track correction by $v + k_{soft}$, which cancels the v of the yaw-rate equation

(b) The steering rack responds faster at high speed, which offsets the larger yaw rate per degree

(c) The curvature feedforward grows with speed and supplies the part of the correction the gain lacks

(d) The heading pole $-v/L$ stays at one place at every speed and sets the speed of the recovery

2.2 Concept check · 1 min

A programmer measures the heading error against the road direction at the front-axle projection instead of under the rear axle, and leaves the curvature feedforward on. What does the car do in the 200 m corner of scenario 2 at 25 m/s?

(a) It holds the line with zero error, because the heading term and the feedforward then agree

(b) It settles about 0.31 m inside the bend, because $\arctan(L\kappa)$ is counted twice

(c) It settles about 0.31 m outside the bend, as with the feedforward switched off

(d) It settles about 0.63 m outside the bend, because the two errors add

2.3 Concept check · 2 min

In scenario 8, the car meets a 25 m corner at 10 m/s with the steering limited to 6°. Raising the cross-track gain from 2 to 12/s has which effect?

(a) The peak error falls in proportion to $1/k_e$, as the misalignment offset does

(b) The loop becomes unstable, because the rack lag sets a finite critical gain at this speed

(c) The peak error hardly changes, while the time on the end stop and out of the lane grows

(d) The peak error falls into the lane band once the gain passes 6/s

2.4 Theory and calculation · 6 min

The default car has $L = 2.9\,\text{m}$, $k_e = 1.2/\text{s}$ and $k_{soft} = 1.0\,\text{m/s}$, with an instantaneous actuator.

(a) Find the time constant of the cross-track decay at 10 and at 30 m/s. *Checkpoint:* 0.917 s and 0.861 s.

(b) Find the heading pole at both speeds, and the ratio of the heading pole to the cross-track pole at each. *Checkpoint:* -3.45 and -10.34/s; ratios 3.16 and 8.91.

(c) Find the time constant at every speed with $k_{soft} = 0$, and say what the softening constant buys at the price of the speed dependence. *Checkpoint:* 0.833 s at every speed.

2.5 Theory and calculation · 7 min

The challenge course holds a corner of $R = 140\,\text{m}$ at $v = 20\,\text{m/s}$ with a misalignment $\delta_{bias} = 0.6°$. The wheelbase is $L = 2.9\,\text{m}$, and the target band is $\pm 0.25\,\text{m}$.

(a) With the shipped tuning, $k_e = 0.5/\text{s}$ and $k_{soft} = 4.0\,\text{m/s}$ with the feedforward off, find the offset in the corner from the missing feedforward. *Checkpoint:* 0.994 m.

(b) With the same tuning, find the size of the offset from the misalignment. *Checkpoint:* 0.503 m.

(c) With the feedforward on and $k_{soft} = 1.0\,\text{m/s}$, find the smallest k_e at which the misalignment offset alone fits the band, and its size at the suggested $k_e = 2.6/\text{s}$. *Checkpoint:* 0.88/s; 0.085 m.

2.6 Theory and calculation · 7 min

Equation (2.14) gives the stability limit of the linearized loop with the rack lag τ_δ. Take $L = 2.9\,\text{m}$ and $k_{soft} = 1.0\,\text{m/s}$.

(a) Find the speed below which no cross-track gain destabilizes the loop, for the default rack of 0.10 s and for the slow rack of 0.45 s. *Checkpoint:* 29 m/s and 6.44 m/s.

(b) For the slow rack at 25 m/s, find $k^*_{e,crit}$, the gain the reader would enter, and the period of the oscillation at the limit. *Checkpoint:* 2.99, 3.11/s and 1.24 s.

(c) The app, with its 50 Hz controller, loses stability between $k_e = 2.55$ and 2.6. By what fraction is the sampled limit below the continuous one, and what causes the gap? *Checkpoint:* About 16 %.

2.7 App challenge · 7 min

Load scenario 2, Constant-radius turn (R = 200 m), with the default seed.

(a) Run 40 s as loaded and export the CSV file. Read the lane IAE on the scorecard and the `steering_deg` and `cross_track_error_m` columns in the row at 30 s, inside the corner. *Checkpoint:* IAE 0.028 m s, steering 0.831°, error 0.000 m, each within one unit of the last digit.

(b) Set Curvature feedforward to Off, press Reset, run 40 s again and read the same three values. *Checkpoint:* IAE 8.797 m s, steering 0.830°, error 0.314 m, each within one unit of the last digit.

(c) Compare the error of part (b) with Equation (2.11), and explain why the steering angle is the same in both runs. *Checkpoint:* 0.314 m predicted.

2.8 App challenge · 8 min

Load scenario 9, Slow steering actuator ($\tau_\delta = 0.45$ s), with the default seed. A playback speed of 5 suits the long run.

(a) Run 40 s as loaded ($k_e = 1.2$) and read the Peak $|e_{ct}|$ and Out of lane tiles. *Checkpoint:* 0.13 m and 0.0 %.

(b) Press Reset, set Cross-track gain to 3 before Run, and run to 40 s. Read the same tiles. *Checkpoint:* 0.46 m and 0.0 %.

(c) Continue the same run to 60 s and export the CSV file. Find the first row in which `lane_departure` is 1, and read the Peak $|e_{ct}|$ tile. *Checkpoint:* 44.7 s, within 0.1 s; more than 1 m (about 61 m).

2.9 App challenge · 9 min

Load scenario 11, The same gain at 30 m/s, or a model that knows the speed, with the default seed. The exported file begins with comment lines that start with #.

(a) Run 40 s as loaded, with Steering on MPC at 30 m/s. Read the Peak $|e_{ct}|$ tile and the lane IAE on the scorecard, and the `mpc_offset_est_deg` column in the row at 20 s. *Checkpoint:* 0.09 m, 0.326 m s within 0.002, and 0.499°.

(b) Set Steering to Stanley, press Reset and run 40 s. Read the lane IAE and `cross_track_error_m` at 20 s, and compare the error with Equation (2.12). *Checkpoint:* 8.850 m s within 0.002, and –0.225 m against 0.2254 m predicted.

(c) Set Speed setpoint to 10 m/s, press Reset and run 40 s under Stanley. In the row at 40 s, read the column `cross_track_error_m`, and explain the ratio of the two standing errors. *Checkpoint:* –0.080 m; ratio 2.82.

2.10 Application area · 3 min

The kinematic bicycle is a fair model up to roughly 0.4 g of lateral acceleration.

(a) Find $v^2\kappa$ for the 200 m corner at 25 m/s, for the peak curvature $2\pi \cdot 3.5/60^2$ of the lane change at 25 and at 30 m/s, and for the 25 m corner at 10 m/s. Which exceed 0.4 g? *Checkpoint:* 3.13, 3.82, 5.50 and 4.00 m/s^2; the last two.

(b) What would a real car do in those cases, and which results of the chapter are optimistic for that reason?

2.11 Application area · 4 min

Highway designers join straights to arcs with transition spirals.

(a) The sudden-curvature road steps from a straight into $R = 120$ m. Find the steering angle the feedforward then demands at once. *Checkpoint:* 1.384°.

(b) In a 30 m spiral into $R = 150$ m at 25 m/s, find the rate at which the required angle moves, using $\mathrm{d}\delta/\mathrm{d}t \approx vL\,\mathrm{d}\kappa/\mathrm{d}s$, and the lag this leaves behind a rack of 0.1 s. *Checkpoint:* 0.92 °/s; 0.09°.

(c) A production lane-keeping assist limits its steering torque well below what the rack can deliver. Give the reason, and say what modeling that limit as an angle limit leaves out.

2.12 Review the agent · 5 min

An AI assistant is asked to tighten the lane keeping in scenario 10, Noisy cross-track measurement ($\sigma_{gps} = 0.25\,\mathrm{m}$ on the gentle sweep at 25 m/s), and replies as follows. “With the default rack, $\tau_\delta v = 2.5\,\mathrm{m}$ is less than $L = 2.9\,\mathrm{m}$, so by the Routh condition of the cubic no cross-track gain can destabilize this loop. Raise k_e from 1.2 to 4/s. Every offset in the Stanley loop falls as $1/k_e$, so the tracking error will fall by more than three times, and the loop stays stable.” Find the flaw and say how you would check it.